
Article:
Kaminska, J., Rzepnikowska, W., Polak, A. et al. (9 more authors) (2016) Phosphatidylinositol-3-phosphate regulates response of cells to proteotoxic stress. The International Journal of Biochemistry & Cell Biology, 79. pp. 494-504. ISSN 1357-2725

https://doi.org/10.1016/j.biocel.2016.08.007

Phosphatidylinositol-3-phosphate regulates response of cells to proteotoxic stress

Joanna Kaminska[a], Weronika Rzepnikowska[a], Anna Polak[a,1], Krzysztof Flis[a], Piotr Soczewka[a], Katarzyna Bala[a], Marzena Sienko[a], Marcin Grynberg[a], Pawel Kaliszewski[a,2], Agnieszka Urbanek[b,3], Kathryn Ayscough[b], Teresa Zoladek[a,*]

[a], Institute of Biochemistry and Biophysics, Polish Academy of Sciences, Pawinskiego 5a, 02-106 Warsaw, Poland

[b], Department of Biomedical Science, University of Sheffield, Sheffield, UK

[1], Present address: Institute of Hematology and Transfusion Medicine, Warsaw, Poland

[2], Present address: Institute of Sport, Warsaw, Poland

[3], Present address: University of York, Wentworth Way, York, UK

*Address correspondence to: Teresa Zoladek, Department of Genetics, Institute of Biochemistry and Biophysics, Polish Academy of Sciences, Pawinskiego 5a, 02-106 Warsaw, Poland, Tel. (48 22) 592-1304; Fax. (48 22) 658-4636; e-mail: teresa@ibb.waw.pl

e-mail addresses: kaminska@ibb.waw.pl (J. Kaminska); wr@ibb.waw.pl (W. Rzepnikowska); polak_anna@wp.pl (A. Polak); kflis@bp.onet.pl (K. Flis); piotrsoczewka92@gmail.com (P. Soczewka); balak@ibb.waw.pl (K. Bala); marsi@ibb.waw.pl (M. Sienko); mr.cingg@gmail.com (M. Grynberg); pawel.kaliszewski@insp.waw.pl (P. Kaliszewski); aga.urbanek@york.ac.uk (A. Urbanek); k.ayscough@sheffield.ac.uk (K. Ayscough).

Acknowledgements: T.Z. lab is a partner in COST ACTION BM1307 PROTEOSTASIS and this work was supported by grant UMO-2011/03/B/NZ1/00570 from the National Science Centre, Poland.

Key words: yeast; human Nedd4 ligase; ubiquitinated proteins; Atg2 (Ynl242w), Atg14 (Ybr128c) and Atg18 (Yfr021w) autophagy proteins; protein aggregates; phosphatidylinositol lipids.

Highlights:

1. Human Nedd4w4 in yeast causes excessive ubiquitination and proteotoxic stress.
2. Proteins accumulate in deposits containing actin filaments, Hsp42 and Hsp104.
3. Toxicity of Nedd4w4 depends on Atg14 subunit of PI3K, Atg18, and Atg2 fragments.
4. Atg2-C fragment contains APT1 domain and this domain binds PI3P.
5. PI3P regulates proteotoxic stress.

Word count: 5620 without references and figure captions.

Abstract

Human Nedd4 ubiquitin ligase, or its variants, inhibit yeast cell growth by disturbing the actin cytoskeleton organization and dynamics, and lead to an increase in levels of ubiquitinated proteins. In a screen for multicopy suppressors which rescue growth of yeast cells producing Nedd4 ligase with an inactive WW4 domain (Nedd4w4), we identified a fragment of ATG2 gene encoding part of the Atg2 core autophagy protein. Expression of the Atg2-C1 fragment (aa 1074-1447) improved growth, actin cytoskeleton organization, but did not significantly change the levels of ubiquitinated proteins in these cells. The GFP-Atg2-C1 protein in Nedd4w4-producing cells primarily localized to a single defined structure adjacent to the vacuole, surrounded by an actin filament ring, containing Hsp42 and Hsp104 chaperones. This localization was not affected in several atg deletion mutants, suggesting that it might be distinct from the phagophore assembly site (PAS). However, deletion of ATG18 encoding a phosphatidylinositol-3-phosphate (PI3P)-binding protein affected the morphology of the GFP-Atg2-C1 structure while deletion of ATG14 encoding a subunit of PI3 kinase suppressed toxicity of Nedd4w4 independently of GFP-Atg2-C1. Further analysis of the Atg2-C1 revealed that it contains an APT1 domain of previously uncharacterized function. Most importantly, we showed that this domain is able to bind phosphatidylinositol phosphates, especially PI3P, which is abundant in the PAS and endosomes. Together our results suggest that human Nedd4 ubiquitinates proteins in yeast and causes proteotoxic stress and, with some Atg proteins, leads to formation of a perivacuolar structure, which may be involved in sequestration, aggregation or degradation of proteins.

1. Introduction

In all environmental and stress conditions the cells need to maintain a balance between protein synthesis and degradation, a state referred to as proteostasis. There are two main routes of protein degradation, autophagy and the ubiquitin proteasome pathway (UPS). Proteins are also degraded in the vacuole when directed there from the plasma membrane via endocytosis or from the Golgi apparatus via the Golgi-to-vacuole pathway (Belgareh-Touze et al., 2008; Lauwers et al., 2010). Proteotoxic stress caused by defects of the proteasome, production of aggregation-prone proteins or malfunction in autophagy leads to formation of protein aggregates, deposits or sequestering bodies, disturbs cell functions and is associated with various pathologies in humans, including neurodegenerative diseases and cancer (Ciechanover, 2013). Mechanisms of abnormal protein sequestering body formation are not well understood.

In the UPS and endocytosis pathways, proteins destined for degradation are marked by a small protein ubiquitin. Ubiquitin, or ubiquitin chains, are attached to these proteins by the consecutive action of a ubiquitin activating enzyme, ubiquitin conjugating enzymes, and ubiquitin ligases. The Nedd4 family of ligases has a C2-WW(1-4)-HECT domain structure, with the C2 domain binding phospholipids, the WW domains interacting with proteins, and the catalytic HECT domain. Human Nedd4 ubiquitin ligase is involved in the endocytic regulation of plasma membrane transporters and receptors (Rotin and Kumar, 2009). Similarly in yeast, the Rsp5 ligase from Nedd4 family regulates numerous cellular processes (Kaliszewski and Zoladek, 2008), including endocytosis and multivesicular body sorting (Lauwers et al., 2010). Moreover, Rsp5 in yeast and Nedd4 in mammalian cells are also involved in the ubiquitination and degradation of misfolded cytosolic proteins upon heat shock (Fang et al., 2014). Nedd4 is associated with several human pathologies by ubiquitination of tumor suppressor proteins (Boase and Kumar, 2015), and α-synuclein, which accumulates in neurons of patients suffering from Parkinson's disease (PD) (Tofaris et al., 2011). Expression of Nedd4 or its variants with mutant WW1 or WW4 domains inhibits yeast cell growth (Gajewska et al., 2003). Growth defect of Nedd4w1-producing cells results from the block of expression of essential OLE1 gene encoding desaturase of fatty acids (Shcherbik et al., 2002). Growth defect of Nedd4w4-producing cells is caused, at least partially, by a disturbance of actin cytoskeleton organization and dynamics (Stawiecka-Mirota et al., 2008). Both, overproduced Rsp5 and ectopically produced Nedd4w4, affect the level of Las17, an activator of the Arp2/3 actin nucleating complex in yeast (Kaminska et al., 2011; Stawiecka-Mirota et al., 2008).

Autophagy is the other mechanism involved in proteostasis. It delivers bulk cytosol, superfluous or damaged organelles and abnormal protein aggregates to the vacuole for degradation (Klionsky and Ohsumi, 1999; Mizushima et al., 2011). Autophagy is a key in the

cell response to stress, in cell differentiation, and contributes to pathogen defense (Lee and Iwasaki, 2008; Sanjuan and Green, 2008) and tumorigenesis (Chen and Debnath, 2010; Mizushima et al., 2008). In yeast the autophagic machinery is quite well known, with 41 proteins encoded by autophagy related genes (ATG) identified (Wen and Klionsky, 2016). Several of these proteins, including Atg2, a peripheral membrane protein (Shintani et al., 2001; Wang et al., 2001), form a core machinery which is needed for all types of autophagy and localize to the preautophagosomal structure or phagophore assembly site (PAS) (Suzuki and Ohsumi, 2010). Efficient localization of Atg2 to the PAS is dependent on a membrane protein Atg9 and a lipid-binding protein Atg18 (Suzuki et al., 2001; Suzuki et al., 2007; Wang et al., 2001). Atg2 forms a complex with Atg18 (Obara et al., 2008) which recently have been shown to localize to the growing edge of the phagophore emerging from the PAS (Suzuki et al., 2013). Atg2-Atg18 complex binds autophagic membranes via phosphatidylinositol-3-phosphate PI3P (Watanabe et al., 2012). PI3P is required for autophagy and is synthesized by the Vps34 PI3 kinase complex which contains the Atg14 subunit recruiting it to the PAS (Obara and Ohsumi, 2011). In addition to the non-selective bulk autophagy induced by starvation, selective autophagic pathways operate in various conditions. Recent studies have identified ubiquitination signals for some types of selective autophagic degradation and specific receptors linking the ubiquitinated cargo and components of the PAS (Johansen and Lamark, 2011; Shaid et al., 2013). Trafficking pathways use several protein complexes for effective clustering of selected cargo to a defined localization in the cell, for example chaperones, which bind misfolded proteins, direct them for proteasomal or autophagic degradation (Khaminets et al., 2015).

To dissect the mechanism of the Nedd4w4 toxicity in yeast and to gain insight into how cells deal with proteotoxic stress, we screened a yeast genomic library for multicopy suppressors restoring growth of NEDD4w4-expressing cells. Among other genes we found a fragment of the ATG2 which encodes Atg2, a core autophagy protein. Further, we studied how deletion of several other ATG genes or overexpression of chaperone genes affects Nedd4w4 toxicity. We have found that PI3P is important in regulation of protein ubiquitination and degradation or sequestration through formation of perivaculoar or cytoplasmic structures.

2. Materials and Methods

2.1. Strains, media and genetic manipulations

E. coli strain DH5α was used for plasmid propagation and BL21(DE3) (Millipore) for protein production. The yeast Saccharomyces cerevisiae strains used in this study are: INV (Invitrogen), PJ69-4A (James et al., 1996), MHY501 (Chen et al., 1993), YYM4 (Stawiecka-Mirota et al., 2008), BY4741, BY4742, BY4741 atg2*Δ*, BY4741 atg13*Δ*, BY4741 atg14*Δ*,

BY4741 atg18*Δ* (Open Biosystems), BY4741 LAS17-GFP (Invitrogen), CRY2040 HSP104-yTagRFP-T and CRY2041 HSP42-yTagRFP-T (Malcova et al., 2016).

Yeast media used were YPD (1% yeast extract, 1% peptone, 2% glucose), SC synthetic complete medium (0.67% yeast nitrogen base without amino acids, 2% glucose) with desired supplements (adenine, uracil, amino acids (aa)); SCgal contains 2% galactose, and SCraf contains 2% raffinose instead of glucose.

To compare the growth of strains, middle-log phase cultures were diluted with water to have 1 OD_{600} equivalents/ml. Aliquots of five-fold serial dilutions of these cell suspensions were spotted onto the medium and incubated as indicated.

Multicopy suppressor screen for DNA fragments restoring growth of yeast cells bearing pYES-NEDD4w4 (with URA3 marker) (Gajewska et al., 2003) was performed using a yeast genomic library from ura3 strain on the YEp351 multicopy plasmid (gift of M. Wysocka-Kapcinska, IBB PAS).

2.2. Plasmids and plasmid construction

Plasmids used and plasmids constructed in this study are described in supplementary data.

2.3. Western blot analysis

Protein extracts were prepared by alkaline lysis (Gajewska et al., 2003) or glass beads metod (Kaminska et al., 2002). Samples were analyzed by Western blotting using mouse monoclonal anti-HA (12CA5, Covance), anti-GFP (Roche), anti-ubiquitin (FK2, Millipore; P4D1, Santa Cruz Biotechnology, Inc.), and anti-3-phosphoglycerate kinase (Pgk1, Thermo Fisher Scientific) antibodies, rabbit polyclonal anti-Nedd4 WW2 domain (No. 07-049, Millipore) and anti-Ape1 (gift of D. Klionsky), anti-glutathione-S-transferase (GST) peroxidase-cojugated (Sigma-Aldrich) and secondary anti-mouse or anti-rabbit IgG horseradish peroxidase-conjugated antibody (Dako) was followed by enhanced chemiluminescence (Millipore or Thermo Fisher Scientific). Proteins were quantified by Image Quant and analyzed statistically by Student t test.

2.4. Actin staining, fluorescence and confocal microscopy

For actin cytoskeleton staining, we employed a previously published procedure (Kaminska et al., 2002). Briefly, cells were grown, fixed and then stained with Alexa Fluor 546-conjugated phalloidin (Thermo Fisher Scientific) for 2 h. Three independent experiments were performed and at least 100 dividing cells of each strain were scored for actin cytoskeleton

organization. For the observation of GFP fusion proteins, the cells were grown at 28°C to logarithmic phase in SC medium. Cells were viewed with an Eclipse E800 (Nikon, Tokyo, Japan) fluorescence microscope equipped with a DS-5Mc camera (Nikon). Images were collected using Lucia General 5.1 software (Laboratory Imaging Ltd.). The same fields were viewed by differential interference contrast (DIC) optics.

For FM4-64 (N-(3-Triethylammoniumpropyl)-4-(6-(4-(Diethylamino) Phenyl) Hexatrienyl) Pyridinium Dibromide; Thermo Fisher Scientific) dye uptake and Cell Tracker Blue CMAC (7-amino-4-chloromethylcoumarin; Thermo Fisher Scientific) staining the cells were grown overnight in SCraf-ura-leu, transferred to SCgal-ura-leu and incubated at 28°C for 2.5 h. After that time FM4-64 was added. Cells were incubated on ice for 30 min and washed and incubated at 28°C for 50 min. Then Cell Tracker Blue CMAC was added and cells were incubated for an additional 10 minutes. The uptake of FM4-64 was stopped with the sodium azide and sodium fluoride, cells were washed and viewed under a confocal laser scanning microscope EZ-C1 Eclipse TE2000-E (Nikon) equipped with a Plan Apo 60 × objective (NA 1.4). Images were collected with EZ-C1 confocal V. 3.6 program (Nikon). Images were processed with EC1 Viewer 3.6 and Adobe Photoshop 8.0. Image acquisition and processing were performed in the Laboratory of Confocal and Fluorescence Microscopy, IBB PAS.

Colocalization of GFP-Atg2-C1 and actin or vacuoles was studied in wild type and atg18*Δ* strains with use of a confocal microscope described above.

2.5. Purification of proteins from bacteria for PIP strip assays.

For PIP strip assays, the truncated versions of Atg2 were expressed as N-terminally GST-tagged recombinant proteins in E. coli BL21(DE3) propagated at 30°C in 2×LB medium supplemented with 50 mM HEPES pH 7.4 and 100 µg/ml carbenicillin (Sigma-Aldrich) for plasmid maintenance. Expression was induced at OD_{600} of 0.2 with 0.2 mM IPTG for 4-6 h. Cells were resuspended in phosphate-buffered saline (PBS) with protease inhibitor cocktail (Complete Mini, EDTA-free, Roche) and lysed by sonication. The homogenate was clarified by centrifugation at 20 000 × g for 15 min at 4°C, supplemented with 2% Triton X-100, 1 mM EDTA and 5 mM dithiothreitol (DTT), and incubated with glutathione magnetic beads (88821, Pierce) for 2-3 h at 4°C. After washing as recommended by the supplier, the proteins were eluted with 20 mM reduced glutathione in buffer (100 mM Tris·Cl pH 8.0, 150 mM NaCl, 2 mM EDTA, 2 mM DTT, 0.1% Tween 20) and the purity of eluted proteins was analyzed by SDS-PAGE followed by Coomassie Brilliant Blue staining.

2.6. PIP strip assay

Membrane-immobilized lipids (PIP Strips, P-6001, Echelon Biosciences Inc.) were blocked with 3% fatty acid-free BSA (Sigma-Aldrich) in PBS-T (PBS + 0.1% Tween-20) and then separately incubated overnight at 4°C with 0.5-1 µg/ml of desired GST-tagged protein or GST alone. Bound proteins were detected by immunoblotting with HRP-conjugated anti-GST antibodies (Sigma) using chemiluminescence (Millipore).

2.7. Computation analyses

The domains of Atg2 were characterized using the HHpred program from the Bioinformatics Toolkit at the LMU Munich (http://toolkit.lmb.uni-muenchen.de/hhpred) (Soding et al., 2005). Additional confirmation was obtained with the FFAS03 program (Jaroszewski et al., 2011). Solenoid structure of Atg2 was calculated with REPETITA (http://protein.bio.unipd.it/repetita/) (Marsella et al., 2009).

3. Results and discussion

3.1. Nedd4w4 affects the level of ubiquitinated proteins and fragments of ATG2 gene suppress Nedd4w4-dependent defects.

Expression of human NEDD4w4 with a mutation inactivating the WW4 domain inhibits yeast cell growth and the toxicity of Nedd4w4 depends, at least in part, on its catalytic activity (Stawiecka-Mirota et al., 2008). We therefore hypothesized that Nedd4w4 produced in yeast cells could excessively ubiquitinate some proteins, cause overflow of cell degradation capacity and thus lead to protein accumulation and aggregation. To check this possibility, we tested the level of ubiquitinated proteins in cells producing Nedd4w4. In agreement with our prediction, cells producing Nedd4w4 showed an approximately 3.9-fold increase in the level of ubiquitinated proteins comparing with the control strain (Figure 1A).

To learn more about Nedd4 action and how cells cope with proteotoxic stress and removal of excessive ubiquitinated proteins, we performed a multicopy suppressor screen using a yeast genomic library. Four different genomic regions were isolated as suppressors of the growth defect of Nedd4w4-producing cells, one of which contained a central part of the ATG2 gene encoding amino acids (aa) 313-1108 (Atg2-F) of Atg2, a core autophagy protein (Figure S1A). To learn if full-length ATG2 or other fragments of ATG2 could also suppress the Nedd4w4-dependent growth defect, multicopy plasmids bearing ATG2, ATG2-*Δ*N (encoding aa 321-1592), ATG2-*Δ*C (aa 1-1210), ATG2-*Δ*N*Δ*C (aa 321-1210), ATG2-N (aa 1-320) or ATG2-C (aa 1105-1592) under the control of native ATG2 promoter were constructed (Figure 2) and tested. ATG2-*Δ*N*Δ*C, that overlapps and in fact is longer than ATG2-F, restored the growth of Nedd4w4-producing cells, albeit rather poorly, suggesting that this additional sequence in this

fragment is not vital to restore growth. ATG2-C was a more efficient suppressor of the Nedd4w4-dependent growth defect, while full-length ATG2 and the other fragments tested were inactive as suppressors (Figure 1B).

Wild type cell show polarization of actin cytoskeleton, actin patches are concentrated in the bud and actin cables are oriented towards the bud (Figure 1C). Nedd4w4 causes defects in polarization of actin cytoskeleton in yeast cells (25% of polarized cells compared with 92% in the control strain; Figure 1C,D) in agreement with previous results (Stawiecka-Mirota et al., 2008) and expression of ATG2-*ΔN*Δ*C* or ATG2-C fragment also increased the polarization of Nedd4w4-producing cells in each of four experiments (to about 54% and 52% of cells, respectively) but because of high variability these differences were not statistically significant (Figure 1C,D). On the other hand, ATG2-F did not affect nonselective autophagy in wild type strain (Figure S1B) and the other analyzed fragments of ATG2 did not restore autophagy in the atg2*Δ* strain (Figure S1C,D). These results show that ATG2-F and ATG-C fragments of Atg2 independently suppress the Nedd4w4-dependent growth defect, surprisingly through a mechanism not directly related to the role in autophagy. Lack of suppression by full-length Atg2 indicates that functions of Atg2 domains can be regulated. In further study we focused on analysis of ATG-C fragment.

3.2. GFP-Atg2-C1 localizes to the structure surrounded by actin filaments in NEDD4w4-expressing cells

The strong positive effect of Atg2-C on growth and actin cytoskeleton organization in Nedd4w4-producing cells prompted us to define in more detail the region responsible for the suppression. First we analyzed the domain structure of Atg2 in silico. At the very N terminus, a fragment of 102 aa is similar to the Chorein-N domain (Figure 2) (http://pfam.sanger.ac.uk/family/PF12624). Next is a region of similarity to mitochondrial protein Fmp27 (aa 112-776) which is predicted to form a solenoid structure and the ATG2-CAD domain (aa 784-921), which contains the CAD motif, but its function remains elusive (PF13329). Then we have found region (aa 1122-1328) similar to the APT1 domain. This domain was originally identified in the Golgi apparatus protein Apt1 of maize, involved in the growth of pollen tubes (PF10351) (Xu and Dooner, 2006). The C terminus of Atg2 also contains a region of homology with human homologs hAtg2A and hAtg2C (Romanyuk et al., 2011). It is composed of two ATG-C domains (PF09333) of unknown function. The first domain is truncated and lacks the distal part, while the second one is intact (Figure 2). According to this analysis, the Atg2 fragment which suppresses the Nedd4w4-dependent growth defect (Atg2-C) contains the APT1 domain and two ATG-C domains.

To determine which of these domains is responsible for suppression, three plasmids encoding protein fusions, GFP-Atg2-C1 (aa 1074-1447), GFP-Atg2-C2 (aa 1435-1592) and GFP-Atg2-C3 (aa 1074-1592) (Figure 3A) were constructed and tested. The cells expressing GFP-ATG2-C1 or GFP-ATG2-C3 grew better, although the effect was less pronounced than with a plasmid bearing fragment ATG2-C (Figure 3B, compare with Figure 1B) possibly due to the presence of the GFP moiety or different levels of expression (ATG2 versus GPD promoter) while a plasmid bearing GFP-ATG2-C2 had no effect. These results support the notion that APT1 and the first ATG-C domains of Atg2 are responsible for suppression of Nedd4w4-dependent defects.

To determine whether the level of ubiquitination correlates with toxicity and suppression, we also studied the level of ubiquitinated proteins in cells producing Nedd4w4, GFP-Atg2-C1 or both. We found that in the presence of Nedd4w4 and GFP-Atg2-C1 the level of ubiquitinated proteins was highly variable and not significantly different from that in Nedd4w4-producing cells (Figure 3C). We also compared the level of ubiquitinated proteins in Nedd4w4-producing strain to that producing wild type Nedd4 which is toxic to yeast only when cells are grown at elevated temperature of 37^{o}C (Stawiecka-Mirota et al., 2008). The effect of GFP-Atg2-C1 was also compared. In this set of experiments, which were performed using different method of protein extraction to better solubilize the ubiquitinated proteins, the results were more reproduciblr and clearly show that the presence of wild type Nedd4 causes a significant elevation in the level of ubiquitinated proteins, comparable to that of Nedd4w4 (Figure S2). The presence of GFP-Atg2-C1 did not affect the level of ubiquitination. Thus, toxicity and suppression are not correlated with respect to changes in total ubiquitination level, and other mechanisms must be considered. On the other hand, the subset of Nedd4-dependent ubiquitinated proteins may be different from that of Nedd4w4 because WW domains are involved in substrate recognition.

We have found that the localization of the GFP-Atg2-C1, GFP-Atg2-C2 and GFP-Atg2-C3 fusion proteins in wild type cells correlated with their suppression ability, since both, GFP-Atg2-C1 and GFP-Atg2-C3, localized to punctate structures in the cytoplasm in most cells but GFP-Atg2-C2 was exclusively diffused in the cytoplasm in all cells (Figure 3D). What is more, the observed GFP-Atg2-C1-containing structures were not the PAS, since their localization was not affected in atg deletion mutants, atg13*Δ,* atg14*Δ* and atg18*Δ,* in which the localization of GFP-Atg2 in the PAS or PAS formation is disturbed (Suzuki et al., 2013; Suzuki et al., 2007) (Figure 3E). Additionally, GFP-Atg2-C1 did not affect nonselective autophagy in NEDD4w4-expressing cells (Figure S3). The conclusion that the structure in question is unlikely to be the PAS is also supported by our previous finding that Atg2 N-terminal region seems to be

sufficient for localization to the PAS (aa 1-1187) (Romanyuk et al., 2011) as well as interaction with Atg18 (Atg2-N3 (aa 1-933) and Atg2-ΔC (aa 1-1210); Figure 3F).

Confocal microscopy analysis of cells producing GFP-Atg2-C1 and Nedd4w4 stained with CMAC (labeling the vacuole interior) and FM4-64 (labeling the vacuolar membrane) revealed that 1-5 punctate structures containing GFP-Atg2-C1 were present per cell and at least one of them, usually the largest one, was located perivacuolarly (Figure 4A). Interestingly, we also found that in NEDD4w4-expressing cells the GFP-Atg2-C1 foci were often surrounded by an actin filament ring (Figure 4B). Moreover, Las17, an activator of actin polymerization, tagged with GFP also localized to these actin structures in Nedd4w4-producing cells (Figure 4C) suggesting that actin filaments observed are Las17-dependent. Finally, GFP-Atg2-C1 foci also contained Nedd4w4 N-terminally tagged with mCherry (Figure 4D) indicating the possibility that GFP-Atg2-C1 may affect Nedd4w4 directly. However, mCherry-Nedd4w4 variant was not toxic to yeast (Figure S4). In conclusion, GFP-Atg2-C1 marks a punctate structure which is present in most wild type cells, while in cells producing Nedd4w4 several Atg2-C1-containing structures are associated with actin filaments (clumps) and the actin polymerization-promoting factor Las17. It is known that actin cytoskeleton modulates the aggregation and toxicity of prion proteins and it has been proposed that cytoskeletal structures provide a scaffold for generation of large aggregates promoting prion formation (Ganusova et al., 2006). Thus, the structure we observe may contain aggregated proteins which cannot be degraded. The mechanism of suppression might be related to the ability to build this structure.

3.3. Structure containing GFP-Atg2-C1 also contains chaperones Hsp42 and Hsp104.

Our finding that human Nedd4 promotes growth arrest and causes formation of perivacuolar structures in yeast cells led us to think that these structures could be similar to the formation of insoluble protein deposits (IPOD), or to stress bodies which are formed when cells are exposed to heat (Miller et al., 2015; Saarikangas and Barral, 2015). Damaged or aggregated proteins amassed in the stress bodies for repair, refolding or degradation, are also sequestered in stress bodies to control protein synthesis (Cherkasov et al., 2015) or in the IPOD to prevent their delivery to the daughter cell during cell division (Spokoini et al., 2012). Hsp104 is involved in the formation and solubilization of protein aggregates (Glover and Lindquist, 1998; Saibil, 2013), specifically those located in the IPOD and stress bodies, therefore Hsp104 is a marker of these structures (Miller et al., 2015; Spokoini et al., 2012). Another marker of stress bodies is the small chaperone Hsp42, which was not found in IPOD marked by amyloid protein Rnq1 (Specht et al., 2011). To identify the Nedd4w4-dependent structures, strains producing Hsp104-

RFP or Hsp42-RFP were used (Malcova et al., 2016) and colocalization of GFP-Atg2-C1 with those makers was observed by confocal microscopy. All the GFP-Atg2-C1 punctate structures colocalized with Hsp42-RFP-containing structures and, when more than a single GFP-Atg2-C1 spot was visible, some, always including the largest one, also colocalized with Hsp104-RFP (Figure 5A). These results suggest that the Nedd4w4-dependent structures are not identical in all cells; they possibly evolve over time. Initially, they all contain Hsp42 and later, when they get larger, Hsp104 becomes associated. This observation supports that idea that the Nedd4-dependent structures have characteristics similar to the recently described protein aggregates where misassembled mutant proteasome subunits are stored (Peters et al., 2015).

Finding the chaperones in Nedd4w4-dependent structures prompted us to test HSP104 and other chaperone genes for multicopy suppression of the Nedd4w4-dependent growth defect. HSP104, but not SSB1 which encodes a chaperone involved in the folding of newly-made polypeptides and curing yeast prions (Chacinska et al., 2001), turned out to be a potent multicopy suppressor of the NEDD4w4-dependent growth defect (Figure 5B). This result again suggests that aggregation of proteins is a major reason of the observed growth defect and that HSP104 expression promotes growth presumably via aggregate solubilization.

Collectively, these results suggest that Nedd4w4 expression causes accumulation of protein aggregates which are surrounded by actin filaments, and that Atg2-C1 fragment, which is present in these structures, affects toxicity of these aggregated proteins.

3.4. Atg18 affects the shape of Atg2-C1-actin structures and, together with Atg14, regulates Nedd4w4 toxicity.

Based on the observation that the GFP-Atg2-C1 punctate structures were larger in atg18*Δ* and in some other atg*Δ* compared to those in the wild type cells we studied the shape of the structures and their colocalization with actin filaments by confocal microscopy in atg18*Δ* cells expressing NEDD4w4. Interestingly, the lack of Atg18 by itself did not affect the formation of ring-like actin structures in NEDD4w4-expressing cells but perturbed them when GFP-Atg2-C1 was also present: instead of a ring-like structure, claw-like actin assemblies were observed and GFP-Atg2-C1 formed similar claws instead of a dot (Figure 6A). We noted that atg18*Δ* mutant cells, similarly to isogenic wild type BY4741 cells, both expressing NEDD4w4, were larger when GFP-ATG2-C1 was co-expressed and that effect was not observed in another genetic background (INV strain) (compare Figures 1C and 6A). Thus, lack of Atg18 together with GFP-Atg2-C1 affects the shape of the structure marked by GFP-Atg2-C1 in NEDD4w4-expressing cells. We considered that the altered organization of perivacuolar structures in these conditions may have a cytoprotective function, therefore we further tested how deletions of

ATG18 and other selected ATG genes affect growth and actin cytoskeleton organization upon expression of NEDD4w4 with or without GFP-ATG2-C1. Deletion of atg13*Δ,* a gene encoding a protein important in an early stage of PAS formation, (Suzuki et al., 2007) had no effect on the toxicity of NEDD4w4 nor on its suppression by GFP-ATG2-C1 (Figure 6B). In contrast, the atg14*Δ* and atg18*Δ* mutations individually suppressed the Nedd4w4 toxicity and cell growth was slightly slower in the presence of GFP-ATG2-C1 (Figure 6B). The actin cytoskeleton organization generally reflected the growth of the analyzed strains, although the atg14*Δ* and atg18*Δ* mutants expressing NEDD4w4, or not, which grew similarly as the wild type control, had a lower number of cells with well-organized actin cytoskeleton (Figure 6C and Figure S5). Atg13, Atg14 and Atg18 are all located in the PAS and are required for autophagy. Since only *atg14Δ* and *atg18Δ* mutations were helpful for growth of Nedd4w4 producing cells, thus not blocking autophagy per se but their effect on aggregation of proteins is important.

The effect of atg deletions on the level of ubiquitinated proteins was also studied. The atg13*Δ*, atg14*Δ* and atg18*Δ* strains showed a significantly higher level of ubiquitinated proteins when Nedd4w4 was produced compared with the respective strains bearing empty vector, similarly as wild type strain. Expression of GFP-ATG2-C1 together with NEDD4w4 did not significantly affect the level of ubiquitinated proteins in atg13*Δ* and atg18*Δ* but decreased it in atg14*Δ*, when compared with respective strains expressing NEDD4w4 alone (Figure 7). This latter decrease might be related to the lower level of Nedd4w4 observed in the presence of GFP-Atg2-C1 in atg14*Δ* in these experiments (Figure 7 and S6). These results show again that the elevated level of ubiquitinated proteins does not correlate with growth defect. Possibly growth depends on the aggregation and sequestration of excessive ubiquitinated proteins in the perivacuolar structure, likely IPOD.

Atg14 and Atg18, i.e., a subunit of PI3 kinase responsible for production of PI3P in the PAS (Obara and Ohsumi, 2011) and a PI3P-binding protein (Watanabe et al., 2012), respectively, appear to be critical for Nedd4w4 toxicity. This indicates that phospholipids, especially PI3P, could be engaged in the action of Nedd4w4 in yeast cells. Both Nedd4 and Rsp5 carry the C2 domain, which in Rsp5 has been found to bind PI and all its phosphate derivatives (Dunn et al., 2004). Recently, it was found that the activity of Nedd4 is controlled through an autoinhibitory interaction, and that PI(1,4,5)P_3 and Ca^{2+} compete with the HECT domain for binding to the C2 domain (Escobedo et al., 2014; Mari et al., 2014). Thus, binding of lipids by C2 domain could up-regulate Nedd4 activity. However, phosphorylated derivatives of PI are not only the structural components of biological membranes, but also play a role in signaling via their recruitment to proteins containing phosphoinositide-binding domains (Strahl and Thorner, 2007). PI3P also serves as a precursor for PI(3,5)P_2 synthesis. This is a less

abundant but important signaling molecule regulating numerous pathways. Several putative protein effectors of PI(3,5)P_2 have been identified in yeast (Lu et al., 2012) and Atg18 also binds PI(3,5)P_2 (Dove et al., 2004) and is a key component of the PI(3,5)P_2 signaling network (Efe et al., 2007). Therefore, it is possible that PI(3,5)P_2 is also an important lipid in the context of Nedd4w4 toxicity and may regulate IPOD formation.

3.5. APT1 domain of Atg2 binds phospholipids

Since Atg18 and Atg14, both involved in PI3P metabolism, influence toxicity of Nedd4w4 and the shape of GFP-Atg2-C1 punctate structure surrounded by actin filaments we reasoned that PI3P might be a regulator of Nedd4w4-dependent aggregation process, and that GFP-Atg2-C1 might bind lipids. Although, the in silico analysis did not show classical lipid-binding motifs, we decided to test this hypothesis. We found that recombinant GST-Atg2-C purified from bacteria sedimented with liposomes obtained from bovine brain (Figure S7). To confirm this result and test specificity of this binding we examined the binding of GST-Atg2-C to PIP strips, an immobilized array of common cellular phospholipids (Figure 8). GST-Atg2-C bound strongly and specifically to PI3P. A shorter fragment GST-Atg2-C4, containing only the APT1 domain (aa 1074-1348) fused to GST, bound to PI3P and with lower affinity to PI(3,5)P_2 and PI(4,5)P_2 (Figure 8B). The Atg2-C4 fragment fused to GFP also suppressed growth defect of Nedd4w4-producing cells (Figure 8C).These results validated our hypothesis that GFP-Atg2-C binds membrane lipids and established the APT1 domain of Atg2 as a new PI3P-binding domain. The APT 1 domain is present at the C-terminus of a family of proteins conserved in Eukaryota from yeasts to humans. According to the Pfam database, proteins containing APT1 (686 sequences from 455 species) can be divided into 41 different families on the basis of protein architecture, including two families containing yeast proteins: Fmp27 and Ypr117w. Our analysis has added Atg2 and its homologs to this group of proteins and suggests that these proteins also might bind PI3P.

The ability of APT1 domain of Atg2 to bind PI3P also suggests that one possible mechanism of suppression of the Nedd4w4-mediated toxicity by Atg2-C1 is by titration of this lipid and downregulation of Nedd4w4 activity. Binding of PI3P by Atg2-C1 may also help in formation of protein aggregates which sequester ubiquitinated proteins and this has a cytoprotective effect. The drop in PI3P level in an endosomal system was already linked to enhancement in amyloidogenic processing of amyloid precursor protein (Morel et al., 2013). Finding that APT1 domain of Atg2 binds PI3P has also important implications in the understanding the mechanism of autophagy, where Atg2 protein plays an essential function.

4. Conclusions

We have shown that expression of Nedd4w4 in yeast causes excessive ubiquitination of proteins and proteotoxic stress. These proteins accumulate in deposits which contain actin filaments and chaperones, initially Hsp42 and later also Hsp104. Some of these deposits are located perivacuolarly. Toxicity of ubiquitinated protein aggregates depends on the abundance of PI3P synthesized by autophagy specific PI3 kinase complex containing Atg14 subunit, PI3P-binding protein Atg18, Atg2 fragment containing APT1 domain which also binds PI3P and Atg2 fragments, other than APT1, might also play an important role. It is intriguing that Atg14 and Atg18 collaborate with Nedd4 and with the actin cytoskeleton in building these structures to sequester aggregated ubiquitinated proteins that cannot be degraded. These structures could possibly derive from the endosomes or multivesicular body where ubiquitinated proteins are arrested on their way to the vacuole. In human cells, Nedd4 ubiquitinates α-synuclein, an abundant brain protein which accumulates in intraneuronal inclusions in PD patients (Tofaris et al., 2011). Nedd4-dependent ubiquitination specifies the fate of exogenous and endogenous α-synuclein by targeting it to endosomes. An excessive amount of Nedd4 appears to restrict the transport of extracellularly derived α-synuclein from the endosome to the lysosome because Nedd4 over-expression significantly increases occurrence and size of α-synuclein positive inclusions surrounded by endosomal structures (Sugeno et al., 2014). Elevated levels of Nedd4 were observed in neuroblastoma cells producing α-synuclein and that correlated with increased Nedd4-dependent ubiquitination and degradation of HSF1 master transcription factor controlling expression of genes encoding chaperones (Kim et al., 2016) adding more complexity to the understanding of Nedd4 role in the prototoxic stress and cell response to this stress. Moreover, Nedd4 is a component of α-synuclein inclusions, Lewy bodies, in a cellular model of PD and PD brain lesions (Sugeno et al., 2014). Thus, expression of Nedd4 in yeast cells may be viewed as a useful model to study the formation of inclusions composed of aggregated proteins, in addition to the PD yeast models with ectopic expression of α-synuclein (Sere et al., 2010; Tardiff et al., 2013; Wijayanti et al., 2015) which power of yeast genetics may add important informations. Unraveling the contribution of lipids and signaling pathways in formation of perivacuolar structure containing protein aggregates may help to understand better how protein homeostasis is controlled in eukaryotes and provide further insight into the mechanism of protein ubiquitination and aggregation in humans suffering from diverse neurodegenerative diseases.

5. Acknowledgments

We thank Drs. D. Klionsky for anti-Ape1 antibody, A. Skoneczna, I. Malcova and J. Hasek for strains, M. Kaksonen for plasmid, M. Wysocka-Kapcinska for genomic library and D.

Romanyuk for help with initial experiments. T.Z. lab is a partner in COST ACTION BM1307 PROTEOSTASIS and this work was supported by grant UMO-2011/03/B/NZ1/00570 from the National Science Centre, Poland.

Authors declare no competing interests.
Founding body had no involvement in study design, collection and interpretation of data and writing of the report.

Figure captions

Figure 1. Nedd4w4 affects the level of ubiquitinated proteins and fragments of ATG2 gene suppress Nedd4w4-dependent defects

A. Wild type **(**BY4741) cells transformed with empty plasmid or plasmid carrying NEDD4w4 were grown at 28^{o}C in SCraf and transferred to SCgal for 3.5 h to induce expression of NEDD4w4. Protein extracts were prepared by alkaline lysis. Western blots were developed with anti-ubiquitin, anti-Nedd4 and anti-Pgk1 antibodies. Pgk1 is a loading control.
B. Growth of wild type strain (YYM4) transformed with plasmid bearing NEDD4w4 and empty plasmid or plasmids bearing indicated versions of ATG2 on SC (Glucose) and SCgal (Galactose) after incubation at 30^{o}C for 3-7 days. Strain bearing two empty vectors was used as a control.
C. Wild type strain (INV) transformed with plasmid bearing NEDD4w4 and with empty vector [-] or plasmids expressing ATG2, ATG2-N, ATG2-*Δ*N*Δ*C or ATG2-C was grown on SCraf medium, shifted to SCgal medium for 4 hours, fixed, stained for actin with labeled phalloidin and viewed for fluorescence and by DIC optics.
D. Quantification of results of four experiments performed as in C.

Figure 2. Atg2 is a multidomain protein.

Schematic representation of Atg2 domains and Atg2 deletion variants studied. Atg2 contains Chorein-N domain (black), Fmp27 homology domain (white), ATG-CAD domain (striped), APT1 domain (gray) and ATG-C domains (intact and truncated) (dotted). Atg2 fragments expressed from plasmids are shown as black lines. Ability to suppress Nedd4w4-dependent growth defect is also shown. NT, not tested.

Figure 3. Fragment Atg2-C1 suppresses Nedd4w4-dependent defects, localizes to a punctate structure in wild type and atg mutant cells and is not required for interaction of Atg2 with Atg18 in two-hybrid system.

A. Schematic representation of GFP-Atg2-C1-3 fusion proteins is shown. Domains are as in Figure 2.

B. Wild type cells were transformed with plasmids p415-GFP-ATG2-C1, p415-GFP-ATG2-C2 or p415-GFP-ATG2-C3 and with plasmid carrying NEDD4w4 or empty vector. Growth of transformants was tested on SC (Glucose) and SCgal (Galactose) after incubation at 30^{o}C for 4 days.

C. Wild type **(**YYM4) cells transformed with empty plasmids or plasmids carrying NEDD4w4 or GFP-ATG2-C1 were grown at 28^{o}C in SCraf and transferred to SCgal for 3.5 h to induce expression of NEDD4w4. Protein extracts were prepared by alkaline lysis. Western blots were developed with anti-ubiquitin, anti-Nedd4, anti-GFP and anti-Pgk1 antibodies. Pgk1 is a loading control. Quantification of results obtained in three independent experiments is shown in lower panel. The value obtained for wild type strain bearing empty vector was set to 1.

D. Localization of Atg2 fragments in wild type transformants bearing plasmids encoding GFP fusions with indicated Atg2 fragments shown in A, assessed by fluorescence microscopy and by DIC optics.

E. Localization of GFP-Atg2-C1 in cells devoid of various indicated ATG genes, assessed by fluorescence microscopy and DIC.

F. Atg2-N3 and Atg2-ΔC interact with Atg18 in two-hybrid system. Two-hybrid tester strain (PJ69-4A) was co-transformed with plasmids expressing DNA binding-domain (BD)-fused Atg2 or Atg2 N-terminal fragments (see Figure 2) and Atg18 fused with activating domain (AD) or with empty vectors. Interaction was monitored by the ability of cells to grow on plates lacking histidine and containing 10 mM 3-aminotriazole (SC-his) after 7 days.

Figure 4. Localization of GFP-Atg2-C1 and Las17-GFP in wild type cells expressing NEDD4w4.

A. Wild type (BY4741) cells transformed with plasmids expressing NEDD4w4 and GFP-ATG2-C1 were grown on SCraf, shifted to SCgal medium for 3.5 h, stained with CMAC and FM4-64 to visualize vacuoles, and observed by confocal microscopy.

B. Wild type (BY4741) cells were transformed with plasmids expressing NEDD4w4 or empty vector and GFP-ATG2-C1 or empty vector. Transformants were grown on SCraf medium, shifted to SCgal medium for 3.5 h, fixed, stained with labeled phalloidin, and viewed by confocal microscopy and by DIC optics. Scale bar: 5 μm. Arrows indicate actin ring-like structures.

C. Strain expressing LAS17-GFP from chromosomal locus was transformed with plasmid carrying NEDD4w4 or empty vector. Transformants were grown and stained as in B, and

viewed by fluorescence microscopy and DIC. Arrows indicate Las17-GFP signal in abnormal actin structures.

D. Wild type cells were transformed with plasmids expressing mCherry-NEDD4w4 and GFP-ATG2-C1 or empty vector. Experiment was performed as in B. Scale bar: 10 μm.

Figure 5. Hsp42 and Hsp104 colocalize with GFP-Atg2-C1 in NEDD4w4-expressing cells and HSP104 suppresses of NEDD4w4-dependent growth defect.

A. Strains producing Hsp42-RFP (CRY2041) or Hsp104-RFP (CRY2040) transformed with both NEDD4w4 and GFP-ATG2-C1 carrying plasmids were grown as in Figure 4A and observed by confocal microscopy.

B. Wild type (YYM4) cells were transformed with empty plasmids or plasmids carrying NEDD4w4 and HSP104 or SSB1. Growth of transformants on SC (Glucose) and SCgal (Galactose) after incubation at 30^{o}C for 4 days was tested.

Figure 6. The atg18*Δ* mutation affects shape of Nedd4w4-dependent structure and together with atg14*Δ* mutation both affect growth and organization of actin cytoskeleton in NEDD4w4-expressing cells.

A. Mutation atg18*Δ* affects the structure of actin clumps and localization of GFP-Atg2-C1 in NEDD4w4-expressing BY4741 cells. The atg18*Δ* cells transformed with plasmid bearing NEDD4w4 or empty vector and GFP-ATG2-C1 or empty vector were grown as in Figure 4B, stained with labeled phalloidin and viewed by confocal microscopy. Arrows indicate claws-like actin structures.

B. Wild type, atg13*Δ*, atg14*Δ* and atg18*Δ* mutant cells (BY4741 background) were transformed with plasmid bearing NEDD4w4 or empty vector and GFP-ATG2-C1 or empty vector. Growth of transformants was tested on SC (Glucose) and SCgal (Galactose) after incubation at 30^{o}C for 4 days.

C. The same transformants as in B were grown as in 4B, stained with labeled phalloidin, and viewed by fluorescence microscopy. Quantification of results is shown.

Figure 7. The atg13*Δ*, atg14*Δ* and atg18*Δ* mutations do not affect protein ubiquitination in cells expressing NEDD4w4.

Wild type, atg13*Δ*, atg14*Δ* and atg18*Δ* strains (in BY4741 background) transformed with empty plasmid or plasmids carrying NEDD4w4 or GFP-ATG2-C1 were grown as in Figure 3C. Protein extracts were prepared by glass beads method. Three independent experiments were performed.

Blots were quantified and analyzed statistically, and relative levels of ubiquitinated proteins normalized to Pgk1 are shown. Statistical significances: *, $p < 0.05$; **, $p < 0.005$.

Figure 8. APT1 domain of Atg2 binds PI3P.

A. Atg2-C subfragments were produced and isolated in native conditions from E. coli as GST fusion proteins. Purity and yield of obtained proteins were checked by SDS-PAGE and Coomassie Brilliant Blue staining (left panel). Schematic representation of purified proteins; the domains are marked as in Figure 2 (right panel).

B. Membranes with immobilized lipids (PIP Strips) were incubated with purified GST-Atg2-C variants or with GST alone as a negative control. Bound proteins were detected using HRP-conjugated anti-GST antibodies. LPA, lysophosphatidic acid; LPC, lysophosphatidylcholine; PI, phosphatidylinositol, PI3P, PI3-phosphate; PI4P, PI4-phosphate; PI5P, PI5-phosphate; PE, phosphatidylethanolamine; PC, phosphatidylcholine; S1P, sphingosine 1-phosphate; PI(3,4)P_2, PI(3,4)-bisphosphate; PI(3,5)P_2, PI(3,5)-bisphosphate; PI(4,5)P_2, PI(4,5)-bisphosphate; PI(3,4,5)P_3, PI(3,4,5)-trisphosphate; PA, phosphatidic acid; PS, phosphatidylserine.

C.Growth of wild type strain (BY4741) transformed with plasmid bearing NEDD4w4 and empty plasmid or plasmids bearing GFP-Atg2-C4 on SC (Glucose) and SCgal (Galactose) after incubation at 30^{o}C for 3-5 days. Strain bearing two empty vectors was used as a control.

References

Belgareh-Touze, N., Leon, S., Erpapazoglou, Z., Stawiecka-Mirota, M., Urban-Grimal, D., Haguenauer-Tsapis, R. 2008. Versatile role of the yeast ubiquitin ligase Rsp5p in intracellular trafficking. Biochem Soc Trans. 36, 791-6.

Boase, N. A., Kumar, S. 2015. NEDD4: The founding member of a family of ubiquitin-protein ligases. Gene. 557, 113-22.

Chacinska, A., Szczesniak, B., Kochneva-Pervukhova, N. V., Kushnirov, V. V., Ter-Avanesyan, M. D., Boguta, M. 2001. Ssb1 chaperone is a [PSI+] prion-curing factor. Curr Genet. 39, 62-7.

Chen, N., Debnath, J. 2010. Autophagy and tumorigenesis. FEBS Lett. 584, 1427-35.

Chen, P., Johnson, P., Sommer, T., Jentsch, S., Hochstrasser, M. 1993. Multiple ubiquitin-conjugating enzymes participate in the in vivo degradation of the yeast MAT alpha 2 repressor. Cell. 74, 357-69.

Cherkasov, V., Grousl, T., Theer, P., Vainshtein, Y., Glasser, C., Mongis, C., Kramer, G., Stoecklin, G., Knop, M., Mogk, A., Bukau, B. 2015. Systemic control of protein

synthesis through sequestration of translation and ribosome biogenesis factors during severe heat stress. FEBS Lett. 589, 3654-64.

Ciechanover, A. 2013. Intracellular protein degradation: from a vague idea through the lysosome and the ubiquitin-proteasome system and onto human diseases and drug targeting. Bioorg Med Chem. 21, 3400-10.

Dove, S. K., Piper, R. C., McEwen, R. K., Yu, J. W., King, M. C., Hughes, D. C., Thuring, J., Holmes, A. B., Cooke, F. T., Michell, R. H., Parker, P. J., Lemmon, M. A. 2004. Svp1p defines a family of phosphatidylinositol 3,5-bisphosphate effectors. Embo J. 23, 1922-33.

Dunn, R., Klos, D. A., Adler, A. S., Hicke, L. 2004. The C2 domain of the Rsp5 ubiquitin ligase binds membrane phosphoinositides and directs ubiquitination of endosomal cargo. J Cell Biol. 165, 135-44.

Efe, J. A., Botelho, R. J., Emr, S. D. 2007. Atg18 regulates organelle morphology and Fab1 kinase activity independent of its membrane recruitment by phosphatidylinositol 3,5-bisphosphate. Mol Biol Cell. 18, 4232-44.

Escobedo, A., Gomes, T., Aragon, E., Martin-Malpartida, P., Ruiz, L., Macias, M. J. 2014. Structural basis of the activation and degradation mechanisms of the E3 ubiquitin ligase Nedd4L. Structure. 22, 1446-57.

Fang, N. N., Chan, G. T., Zhu, M., Comyn, S. A., Persaud, A., Deshaies, R. J., Rotin, D., Gsponer, J., Mayor, T. 2014. Rsp5/Nedd4 is the main ubiquitin ligase that targets cytosolic misfolded proteins following heat stress. Nat Cell Biol. 16, 1227-37.

Gajewska, B., Shcherbik, N., Oficjalska, D., Haines, D. S., Zoladek, T. 2003. Functional analysis of the human orthologue of the RSP5-encoded ubiquitin protein ligase, hNedd4, in yeast. Curr Genet. 43, 1-10.

Ganusova, E. E., Ozolins, L. N., Bhagat, S., Newnam, G. P., Wegrzyn, R. D., Sherman, M. Y., Chernoff, Y. O. 2006. Modulation of prion formation, aggregation, and toxicity by the actin cytoskeleton in yeast. Mol Cell Biol. 26, 617-29.

Glover, J. R., Lindquist, S. 1998. Hsp104, Hsp70, and Hsp40: a novel chaperone system that rescues previously aggregated proteins. Cell. 94, 73-82.

James, P., Halladay, J., Craig, E. A. 1996. Genomic libraries and a host strain designed for highly efficient two-hybrid selection in yeast. Genetics. 144, 1425-36.

Jaroszewski, L., Li, Z., Cai, X. H., Weber, C., Godzik, A. 2011. FFAS server: novel features and applications. Nucleic Acids Res. 39, W38-44.

Johansen, T., Lamark, T. 2011. Selective autophagy mediated by autophagic adapter proteins. Autophagy. 7, 279-96.

Kaliszewski, P., Zoladek, T. 2008. The role of Rsp5 ubiquitin ligase in regulation of diverse processes in yeast cells. Acta Biochim Pol. 55, 649-62.

Kaminska, J., Gajewska, B., Hopper, A. K., Zoladek, T. 2002. Rsp5p, a new link between the actin cytoskeleton and endocytosis in the yeast Saccharomyces cerevisiae. Mol Cell Biol. 22, 6946-8.

Kaminska, J., Spiess, M., Stawiecka-Mirota, M., Monkaityte, R., Haguenauer-Tsapis, R., Urban-Grimal, D., Winsor, B., Zoladek, T. 2011. Yeast Rsp5 ubiquitin ligase affects the actin cytoskeleton in vivo and in vitro. Eur J Cell Biol. 90, 1016-28.

Khaminets, A., Behl, C., Dikic, I. 2015. Ubiquitin-Dependent And Independent Signals In Selective Autophagy. Trends Cell Biol.

Kim, E., Wang, B., Sastry, N., Masliah, E., Nelson, P. T., Cai, H., Liao, F. F. 2016. NEDD4-mediated HSF1 degradation underlies alpha-synucleinopathy. Hum Mol Genet. 25, 211-22.

Klionsky, D. J., Ohsumi, Y. 1999. Vacuolar import of proteins and organelles from the cytoplasm. Annu Rev Cell Dev Biol. 15, 1-32.

Lauwers, E., Erpapazoglou, Z., Haguenauer-Tsapis, R., Andre, B. 2010. The ubiquitin code of yeast permease trafficking. Trends Cell Biol. 20, 196-204.

Lee, H. K., Iwasaki, A. 2008. Autophagy and antiviral immunity. Curr Opin Immunol. 20, 23-9.

Lu, K. Y., Tao, S. C., Yang, T. C., Ho, Y. H., Lee, C. H., Lin, C. C., Juan, H. F., Huang, H. C., Yang, C. Y., Chen, M. S., Lin, Y. Y., Lu, J. Y., Zhu, H., Chen, C. S. 2012. Profiling lipid-protein interactions using nonquenched fluorescent liposomal nanovesicles and proteome microarrays. Mol Cell Proteomics. 11, 1177-90.

Malcova, I., Farkasovsky, M., Senohrabkova, L., Vasicova, P., Hasek, J. 2016. New integrative modules for multicolor-protein labeling and live-cell imaging in Saccharomyces cerevisiae. FEMS Yeast Res.

Mari, S., Ruetalo, N., Maspero, E., Stoffregen, M. C., Pasqualato, S., Polo, S., Wiesner, S. 2014. Structural and functional framework for the autoinhibition of Nedd4-family ubiquitin ligases. Structure. 22, 1639-49.

Marsella, L., Sirocco, F., Trovato, A., Seno, F., Tosatto, S. C. 2009. REPETITA: detection and discrimination of the periodicity of protein solenoid repeats by discrete Fourier transform. Bioinformatics. 25, i289-95.

Miller, S. B., Mogk, A., Bukau, B. 2015. Spatially organized aggregation of misfolded proteins as cellular stress defense strategy. J Mol Biol. 427, 1564-74.

Mizushima, N., Levine, B., Cuervo, A. M., Klionsky, D. J. 2008. Autophagy fights disease through cellular self-digestion. Nature. 451, 1069-75.

Mizushima, N., Yoshimori, T., Ohsumi, Y. 2011. The role of Atg proteins in autophagosome formation. Annu Rev Cell Dev Biol. 27, 107-32.

Morel, E., Chamoun, Z., Lasiecka, Z. M., Chan, R. B., Williamson, R. L., Vetanovetz, C., Dall'Armi, C., Simoes, S., Point Du Jour, K. S., McCabe, B. D., Small, S. A., Di Paolo, G. 2013. Phosphatidylinositol-3-phosphate regulates sorting and processing of amyloid precursor protein through the endosomal system. Nat Commun. 4, 2250.

Obara, K., Ohsumi, Y. 2011. PtdIns 3-Kinase Orchestrates Autophagosome Formation in Yeast. J Lipids. 2011, 498768.

Obara, K., Sekito, T., Niimi, K., Ohsumi, Y. 2008. The Atg18-Atg2 complex is recruited to autophagic membranes via phosphatidylinositol 3-phosphate and exerts an essential function. J Biol Chem. 283, 23972-80.

Peters, L. Z., Karmon, O., David-Kadoch, G., Hazan, R., Yu, T., Glickman, M. H., Ben-Aroya, S. 2015. The protein quality control machinery regulates its misassembled proteasome subunits. PLoS Genet. 11, e1005178.

Romanyuk, D., Polak, A., Maleszewska, A., Sienko, M., Grynberg, M., Zoladek, T. 2011. Human hAtg2A protein expressed in yeast is recruited to preautophagosomal structure but does not complement autophagy defects of atg2Delta strain. Acta Biochim Pol. 58, 365-74.

Rotin, D., Kumar, S. 2009. Physiological functions of the HECT family of ubiquitin ligases. Nat Rev Mol Cell Biol. 10, 398-409.

Saarikangas, J., Barral, Y. 2015. Protein aggregates are associated with replicative aging without compromising protein quality control. Elife. 4, e06197.

Saibil, H. 2013. Chaperone machines for protein folding, unfolding and disaggregation. Nat Rev Mol Cell Biol. 14, 630-42.

Sanjuan, M. A., Green, D. R. 2008. Eating for good health: linking autophagy and phagocytosis in host defense. Autophagy. 4, 607-11.

Sere, Y. Y., Regnacq, M., Colas, J., Berges, T. 2010. A Saccharomyces cerevisiae strain unable to store neutral lipids is tolerant to oxidative stress induced by alpha-synuclein. Free Radic Biol Med. 49, 1755-64.

Shaid, S., Brandts, C. H., Serve, H., Dikic, I. 2013. Ubiquitination and selective autophagy. Cell Death Differ. 20, 21-30.

Shcherbik, N., Kumar, S., Haines, D. S. 2002. Substrate proteolysis is inhibited by dominant-negative Nedd4 and Rsp5 mutants harboring alterations in WW domain 1. J Cell Sci. 115, 1041-8.

Shintani, T., Suzuki, K., Kamada, Y., Noda, T., Ohsumi, Y. 2001. Apg2p functions in autophagosome formation on the perivacuolar structure. J Biol Chem. 276, 30452-60.

Soding, J., Biegert, A., Lupas, A. N. 2005. The HHpred interactive server for protein homology detection and structure prediction. Nucleic Acids Res. 33, W244-8.

Specht, S., Miller, S. B., Mogk, A., Bukau, B. 2011. Hsp42 is required for sequestration of protein aggregates into deposition sites in Saccharomyces cerevisiae. J Cell Biol. 195, 617-29.

Spokoini, R., Moldavski, O., Nahmias, Y., England, J. L., Schuldiner, M., Kaganovich, D. 2012. Confinement to organelle-associated inclusion structures mediates asymmetric inheritance of aggregated protein in budding yeast. Cell Rep. 2, 738-47.

Stawiecka-Mirota, M., Kaminska, J., Urban-Grimal, D., Haines, D. S., Zoladek, T. 2008. Nedd4, a human ubiquitin ligase, affects actin cytoskeleton in yeast cells. Exp Cell Res. 314, 3318-25.

Strahl, T., Thorner, J. 2007. Synthesis and function of membrane phosphoinositides in budding yeast, Saccharomyces cerevisiae. Biochim Biophys Acta. 1771, 353-404.

Sugeno, N., Hasegawa, T., Tanaka, N., Fukuda, M., Wakabayashi, K., Oshima, R., Konno, M., Miura, E., Kikuchi, A., Baba, T., Anan, T., Nakao, M., Geisler, S., Aoki, M., Takeda, A. 2014. Lys-63-linked ubiquitination by E3 ubiquitin ligase Nedd4-1 facilitates endosomal sequestration of internalized alpha-synuclein. J Biol Chem. 289, 18137-51.

Suzuki, K., Akioka, M., Kondo-Kakuta, C., Yamamoto, H., Ohsumi, Y. 2013. Fine mapping of autophagy-related proteins during autophagosome formation in Saccharomyces cerevisiae. J Cell Sci. 126, 2534-44.

Suzuki, K., Kirisako, T., Kamada, Y., Mizushima, N., Noda, T., Ohsumi, Y. 2001. The pre-autophagosomal structure organized by concerted functions of APG genes is essential for autophagosome formation. Embo J. 20, 5971-81.

Suzuki, K., Kubota, Y., Sekito, T., Ohsumi, Y. 2007. Hierarchy of Atg proteins in pre-autophagosomal structure organization. Genes Cells. 12, 209-18.

Suzuki, K., Ohsumi, Y. 2010. Current knowledge of the pre-autophagosomal structure (PAS). FEBS Lett. 584, 1280-6.

Tardiff, D. F., Jui, N. T., Khurana, V., Tambe, M. A., Thompson, M. L., Chung, C. Y., Kamadurai, H. B., Kim, H. T., Lancaster, A. K., Caldwell, K. A., Caldwell, G. A., Rochet, J. C., Buchwald, S. L., Lindquist, S. 2013. Yeast reveal a "druggable" Rsp5/Nedd4 network that ameliorates alpha-synuclein toxicity in neurons. Science. 342, 979-83.

Tofaris, G. K., Kim, H. T., Hourez, R., Jung, J. W., Kim, K. P., Goldberg, A. L. 2011. Ubiquitin ligase Nedd4 promotes alpha-synuclein degradation by the endosomal-lysosomal pathway. Proc Natl Acad Sci U S A. 108, 17004-9.

Wang, C. W., Kim, J., Huang, W. P., Abeliovich, H., Stromhaug, P. E., Dunn, W. A., Jr., Klionsky, D. J. 2001. Apg2 is a novel protein required for the cytoplasm to vacuole targeting, autophagy, and pexophagy pathways. J Biol Chem. 276, 30442-51.

Watanabe, Y., Kobayashi, T., Yamamoto, H., Hoshida, H., Akada, R., Inagaki, F., Ohsumi, Y., Noda, N. N. 2012. Structure-based analyses reveal distinct binding sites for Atg2 and phosphoinositides in Atg18. J Biol Chem. 287, 31681-90.

Wen, X., Klionsky, D. J. 2016. An overview of macroautophagy in yeast. J Mol Biol. 428, 1681-99.

Wijayanti, I., Watanabe, D., Oshiro, S., Takagi, H. 2015. Isolation and functional analysis of yeast ubiquitin ligase Rsp5 variants that alleviate the toxicity of human alpha-synuclein. J Biochem. 157, 251-60.

Xu, Z., Dooner, H. K. 2006. The maize aberrant pollen transmission 1 gene is a SABRE/KIP homolog required for pollen tube growth. Genetics. 172, 1251-61.

FIGURE 1

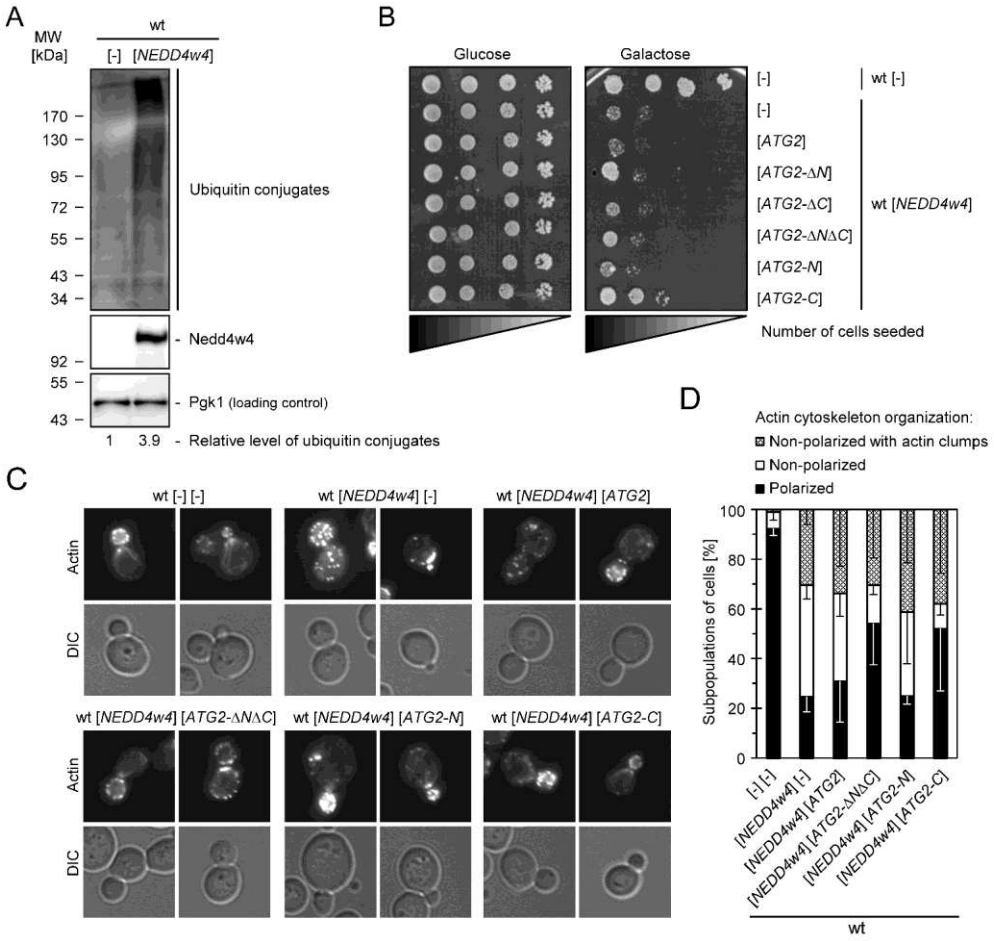
A
MW [kDa]
wt
[-] [NEDD4w4]
170
130
95
72
55
43
34
Ubiquitin conjugates
Nedd4w4
92
55
Pgk1 (loading control)
43
1 3.9 - Relative level of ubiquitin conjugates
B
Glucose
Galactose
[-]
[-]
[ATG2]
[ATG2-ΔN]
[ATG2-ΔC]
[ATG2-ΔNΔC]
[ATG2-N]
[ATG2-C]
wt [-]
wt [NEDD4w4]
Number of cells seeded
C
wt [-] [-]
wt [NEDD4w4] [-]
wt [NEDD4w4] [ATG2]
Actin
DIC
wt [NEDD4w4] [ATG2-ΔNΔC]
wt [NEDD4w4] [ATG2-N]
wt [NEDD4w4] [ATG2-C]
Actin
DIC
D
Actin cytoskeleton organization:
Non-polarized with actin clumps
Non-polarized
Polarized
Subpopulations of cells [%]
100
80
60
40
20
0
[-] [-]
[NEDD4w4] [-]
[NEDD4w4] [ATG2]
[NEDD4w4] [ATG2-ΔNΔC]
[NEDD4w4] [ATG2-N]
[NEDD4w4] [ATG2-C]
wt

FIGURE 2

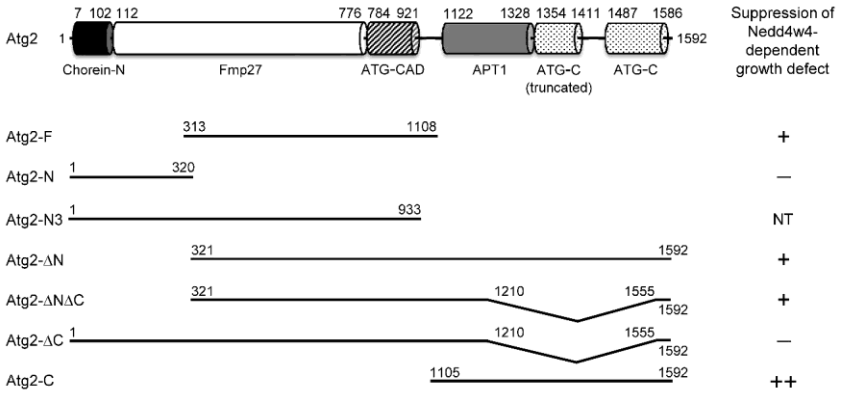
Atg2
1
7 102 112
776 784 921
1122
1328 1354 1411
1487 1586
1592
Chorein-N
Fmp27
ATG-CAD
APT1
ATG-C (truncated)
ATG-C
Suppression of Nedd4w4-dependent growth defect
Atg2-F
313
1108
+
Atg2-N
1
320
–
Atg2-N3
1
933
NT
Atg2-ΔN
321
1592
+
Atg2-ΔNΔC
321
1210
1555
1592
+
Atg2-ΔC
1
1210
1555
1592
–
Atg2-C
1105
1592
++

FIGURE 3

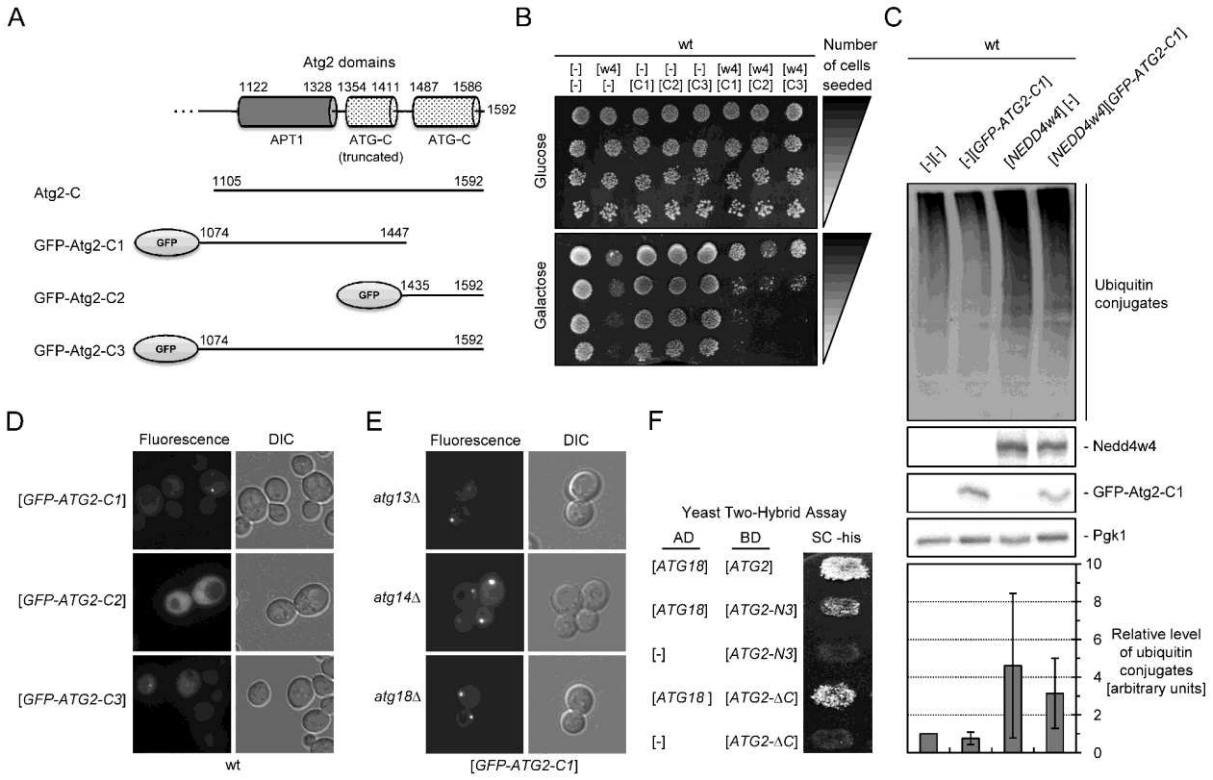
A
Atg2 domains
1122
1328
1354
1411
1487
1586
1592
APT1
ATG-C
(truncated)
ATG-C
Atg2-C
1105
1592
GFP-Atg2-C1
GFP
1074
1447
GFP-Atg2-C2
GFP
1435
1592
GFP-Atg2-C3
GFP
1074
1592
B
wt
[-] [-]
[w4] [-]
[-] [C1]
[-] [C2]
[-] [C3]
[w4] [C1]
[w4] [C2]
[w4] [C3]
Number of cells seeded
Glucose
Galactose
C
wt
[-][-]
[-][GFP-ATG2-C1]
[NEDD4w4][-]
[NEDD4w4][GFP-ATG2-C1]
Ubiquitin conjugates
- Nedd4w4
- GFP-Atg2-C1
- Pgk1
Relative level of ubiquitin conjugates [arbitrary units]
10
8
6
4
2
0
D
Fluorescence
DIC
[GFP-ATG2-C1]
[GFP-ATG2-C2]
[GFP-ATG2-C3]
wt
E
Fluorescence
DIC
atg13Δ
atg14Δ
atg18Δ
[GFP-ATG2-C1]
F
Yeast Two-Hybrid Assay
AD
BD
SC -his
[ATG18] [ATG2]
[ATG18] [ATG2-N3]
[-] [ATG2-N3]
[ATG18] [ATG2-ΔC]
[-] [ATG2-ΔC]

FIGURE 4

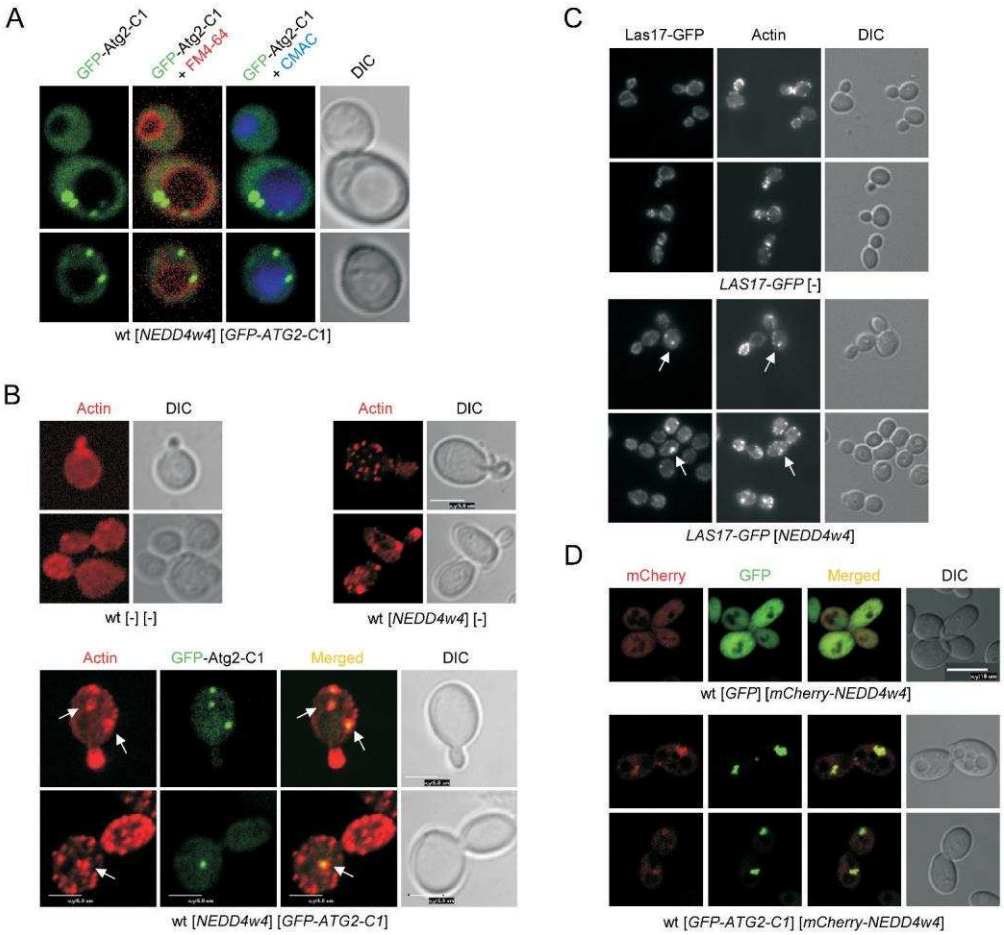
A
GFP-Atg2-C1
GFP-Atg2-C1 + FM4-64
GFP-Atg2-C1 + CMAC
DIC
wt [NEDD4w4] [GFP-ATG2-C1]
B
Actin
DIC
wt [-] [-]
wt [NEDD4w4] [-]
Actin
GFP-Atg2-C1
Merged
DIC
wt [NEDD4w4] [GFP-ATG2-C1]
C
Las17-GFP
Actin
DIC
LAS17-GFP [-]
LAS17-GFP [NEDD4w4]
D
mCherry
GFP
Merged
DIC
wt [GFP] [mCherry-NEDD4w4]
wt [GFP-ATG2-C1] [mCherry-NEDD4w4]

FIGURE 5

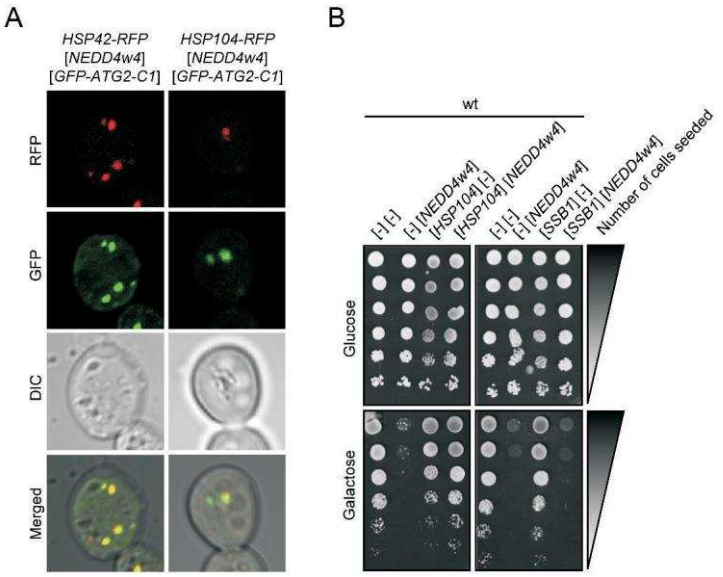
A
HSP42-RFP
[NEDD4w4]
[GFP-ATG2-C1]
HSP104-RFP
[NEDD4w4]
[GFP-ATG2-C1]
RFP
GFP
DIC
Merged
B
wt
[-] [-]
[-] [NEDD4w4]
[HSP104] [-]
[HSP104] [NEDD4w4]
[-] [-]
[-] [NEDD4w4]
[SSB1] [-]
[SSB1] [NEDD4w4]
Number of cells seeded
Glucose
Galactose

FIGURE 6

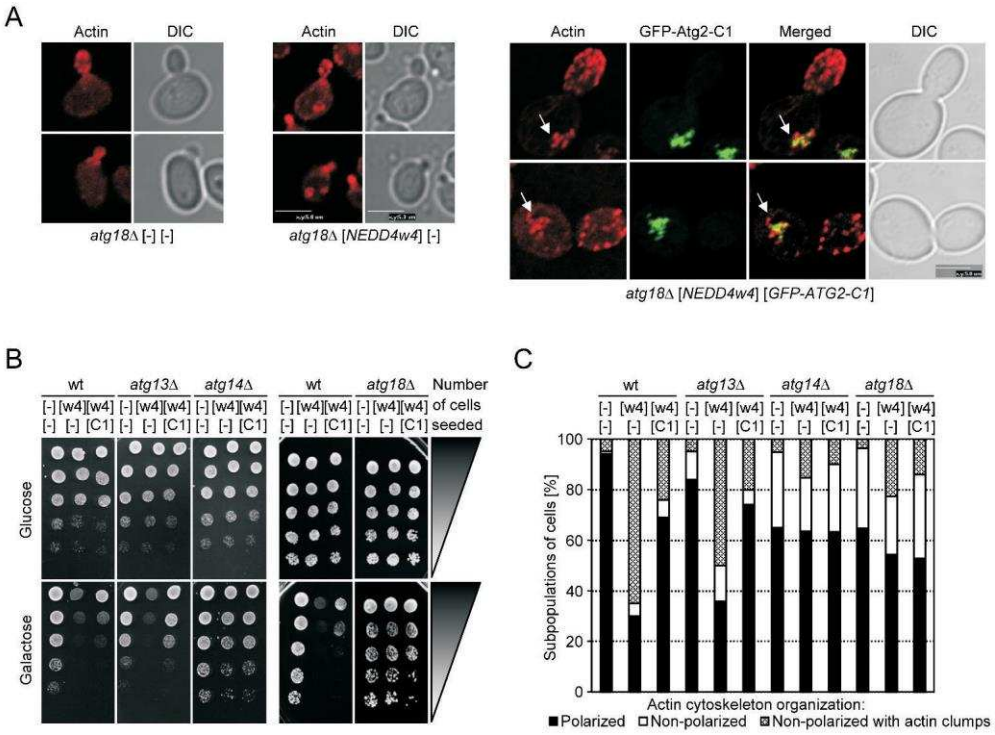
A
Actin
DIC
atg18Δ [-] [-]
atg18Δ [NEDD4w4] [-]
GFP-Atg2-C1
Merged
atg18Δ [NEDD4w4] [GFP-ATG2-C1]
B
wt
atg13Δ
atg14Δ
atg18Δ
Number of cells seeded
Glucose
Galactose
C
Subpopulations of cells [%]
Actin cytoskeleton organization:
Polarized
Non-polarized
Non-polarized with actin clumps

FIGURE 7

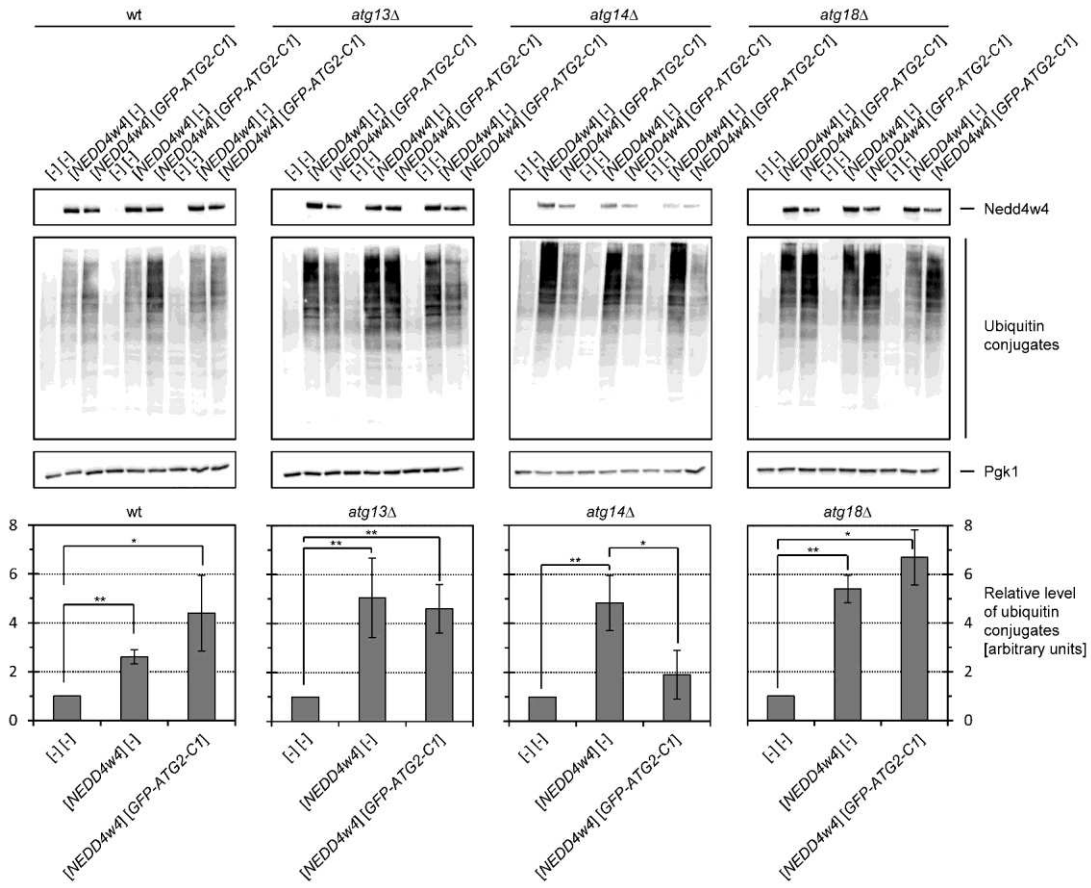
wt
atg13Δ
atg14Δ
atg18Δ
[-] [-]
[NEDD4w4] [-]
[NEDD4w4] [GFP-ATG2-C1]
Nedd4w4
Ubiquitin conjugates
Pgk1
Relative level of ubiquitin conjugates [arbitrary units]
0
2
4
6
8
*
**

FIGURE 8

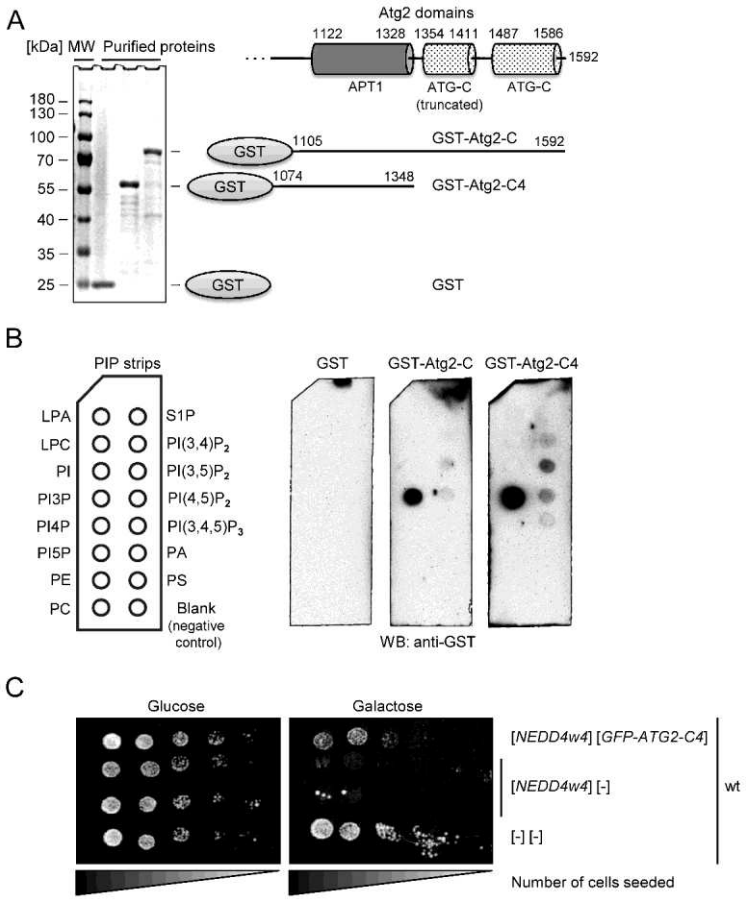
A
[kDa] MW
Purified proteins
180
130
100
70
55
40
35
25
Atg2 domains
1122
1328
1354
1411
1487
1586
1592
APT1
ATG-C
(truncated)
ATG-C
GST
1105
GST-Atg2-C
1592
GST
1074
1348
GST-Atg2-C4
GST
GST
B
PIP strips
LPA
LPC
PI
PI3P
PI4P
PI5P
PE
PC
S1P
PI(3,4)P2
PI(3,5)P2
PI(4,5)P2
PI(3,4,5)P3
PA
PS
Blank
(negative
control)
GST
GST-Atg2-C
GST-Atg2-C4
WB: anti-GST
C
Glucose
Galactose
[NEDD4w4] [GFP-ATG2-C4]
[NEDD4w4] [-]
[-] [-]
wt
Number of cells seeded

SUPPLEMENTARY MATERIALS AND METHODS (Kaminska et al., 2016)

Plasmids and plasmid construction

The plasmids used in this study: YEp351 (Hill et al., 1986); YCp33lac and YEp181lac (Gietz and Sugino, 1988); pGBT9, pGAD424 (TaKaRa Clontech Kusatsu, Shiga, Japan); pYES-NEDD4 and pYES-NEDD4w4 (Gajewska et al., 2003); pGFP-ATG8 (Suzuki et al., 2001); pGEM-ATG2-XS, p415-P_{GPD1}-GFP-ATG2 and pGBT9-ATG2 (Romanyuk et al., 2011); pTS102 bearing ATG2 (Shintani et al., 2001); PS-159 bearing AD-ATG18 fusion (gift from D. Klionsky, University of Michigan, USA); pFL46S-HSP104 and pFL46S-SSB1 (Chacinska et al., 2001).

To test for suppression of the Nedd4w4-dependent growth defect, the plasmid YEp351-ATG2 was constructed by transfer of fragments SphI-SacI and SacI-SacI from pTS102 to YEp351. Then YEp351-ATG2-XS containing XmaI and SalI sites flanking ATG2 ORF was obtained by replacing the wild type fragments with in vitro-mutated fragments of pGEM-ATG2-XS. To construct plasmid expressing ATG2-N fragment (ATG2 promoter and fragment encoding aa 1-320 of Atg2) the PCR product obtained by using specific primers introducing flanking XmaI and SalI sites and YEp351-ATG2 as a template was digested with XmaI and SalI and ligated with YEp351. Plasmid expressing ATG2-C (encoding aa 1105-1592) was constructed similarly, the PCR product containing ATG2-C was obtained by using specific primers introducing flanking XmaI and SalI and was transferred to YEp351, and then the fragment containing promoter amplified using YEp-ATG2-XS as a template was digested with SphI and XmaI and inserted between the SphI and XmaI sites in front of ATG-C. To construct plasmid YEp-ATG2-ΔN, XmaI site and a new ATG codon before codon 320 of ATG2 in the NcoI-BgtZI DNA fragment was introduced by in vitro mutagenesis and the wild type fragment was replaced in YEp-ATG-XS. Then XmaI-XmaI fragment was deleted. YEp-ATG2-ΔC and YEp-ATG2-ΔNΔC were constructed by digestion of YEp351-ATG2 or YEp-ATG2-ΔN with EagI and religation.

Plasmids used for localization and suppression studies, p415-GFP-ATG2-C1, p415-GFP-ATG2-C2, p415-GFP-ATG2-C3 and p415-GFP-ATG2-C4, were constructed by PCR amplification of respective fragments based on plasmid bearing ATG2, digestion with HindIII and SalI and ligation into HindIII/SalI-digested p415-P_{GPD}-GFP.

Plasmids used in two-hybrid experiments, derivatives of pGBT9 and pGAD424, containing ATG2 fragments were constructed similarly as described above. Also plasmids encoding fragment of ATG2 bearing three domains from the Atg2 N terminus, pGAD424-Atg2-N3 and pGBT9-Atg2-N3, were constructed by digestion of pGAD424-Atg2-XS and pGBT9-Atg2-XS with ClaI and SalI, filling ends with Klenow polymerase and religation. The pGBT9-Atg2-ΔC plasmid was constructed by in-frame deletion of 1032-bp EagI-EagI fragment from pGBT9-Atg2-XS.

Plasmids used for protein expression in E. coli are based on the pGEX-4T-1 vector, which is a part of the glutathione S-transferase (GST) gene fusion system from GE Healthcare. The Atg2-C-encoding sequence was subcloned into EcoRI/SalI-linearized pGEX-4T-1 as a 1497-bp EcoRI-SalI fragment of pGBT9-ATG2-C giving pGEX-ATG2-C. The pKF300TU vector was constructed by replacement of the multicloning site (30-bp

BamHI-NotI part) in pGEX-4T-1 with a 105-bp synthetic linker encoding a TEV protease cleavage site followed in-frame by several restriction sites and three STOP codons (BamHI-TEV_c.s.-NdeI-NcoI-XbaI-SpeI-BglII-SmaI-EcoRI-HindIII-ClaI-SalI-XhoI-3×STOP-NotI). A control plasmid, pKF463, containing STOP codon directly downstream of the TEV cleavage site, was created by ligation of a 4978-bp BamHI-EcoRI fragment of pKF300TU and 33-bp BamHI/EcoRI-digested dsDNA specific linker containing the AarI recognition site positioned downstream of the STOP codon. The AarI enzyme is a type IIS endonuclease and allows, in this particular case, the creation of a seamless fusion of a sequence encoding a protein of interest with the TEV cleavage site. The sequence encoding Atg2-S1074-P1348 (isolated APT1 domain) was PCR-amplified from strain S288C genomic DNA with specific primers and cloned as an 843-bp Esp3I-Esp3I fragment into AarI/SalI-linearized pKF463 yielding pKF481.

To observe cellular localization of Nedd4w4, the plasmid pYES-P_{GAL}-mCherry-Nedd4w4 was constructed with the use of fusion PCR. Based on P_{GAL1}-NEDD4w4, two PCR products were obtained: GAL1 promoter and fragment of NEDD4w4 gene. The mCherry encoding sequence was amplified from pFA-mCherry-NatMX plasmid (gift from M. Kaksonen lab,University of Geneva, Switzerland). Three PCR products were mixed and final PCR was performed to get P_{GAL1}-mCherry-NEDD4w4. Obtained DNA was AgeI/BlnI digested and used to replace the AgeI-BlnI fragment of pYES-NEDD4w4.

Purification of proteins from bacteria

For liposome assay and high speed pelleting assay with actin, the Atg2 fragments were purified as follows. Plasmid bearing GST-ATG2-C was transformed into E.coli strain OverExpress™ C43(DE3) (Lucigen Corporation, Middleton, WI, USA). Bacteria were grown to OD600 ~0.6 in 2×YT medium at 37°C. Protein expression was induced by addition of IPTG to 1 mM, then cells were pelleted, resuspended in phosphate-buffered saline (PBS) pH 7.0 and lysed by sonication. Then Triton X-100 was added to 1% and samples were incubated for 30 min at 4°C. After centrifugation 20 min 20 000×g 10 ml supernatant was filtered through Millex filter unit (Millipore) and incubated with 250 µl of glutathione transferase (GST)-beads (GE Healthcare). GST-Atg2-C was eluted using reduced glutathione. Buffer was exchanged using PD Minitrap G-25 columns (GE Healthcare Little Chalfont, UK) into buffer G (2 mM Tris-HCl pH 8.0, 0.2 mM $CaCl_2$, 0.2 mM ATP, 0.5 mM dithiothreitol) or buffer B (20 mM HEPES pH 7.2, 150 mM NaCl).

Liposome assay

For preparation of liposomes, 25 µl of a 25 mg/ml solution of Folch fraction I from bovine brain (Sigma-Aldrich) was dried under nitrogen and resuspended in 250 µl of buffer B (20 mM HEPES pH 7.2, 150 mM NaCl) at 60°C for 1 h. GST-Atg2-C was mixed with 20 µl of liposomes and incubated at room temperature for 30 minutes. Liposomes and bound proteins were pelleted by centrifugation at 250 000 × g for 15 minutes, and samples were analyzed by SDS–PAGE.

Monitoring of authophagy by Pho8Δ60 alkaline phosphatase test

For measurements of autophagic activity, the alkaline phosphatase test was performed as described previously (Noda et al., 1995). Strains KJK146 pho13Δ pho8Δ60 (a pho13Δ derivative of TN125; Shintani et al., 2001) and YPJ2 pho8Δ60 strain (Romanyuk et al., 2011) were used. Four independent experiments were performed.

SUPPLEMENTARY FIGURES

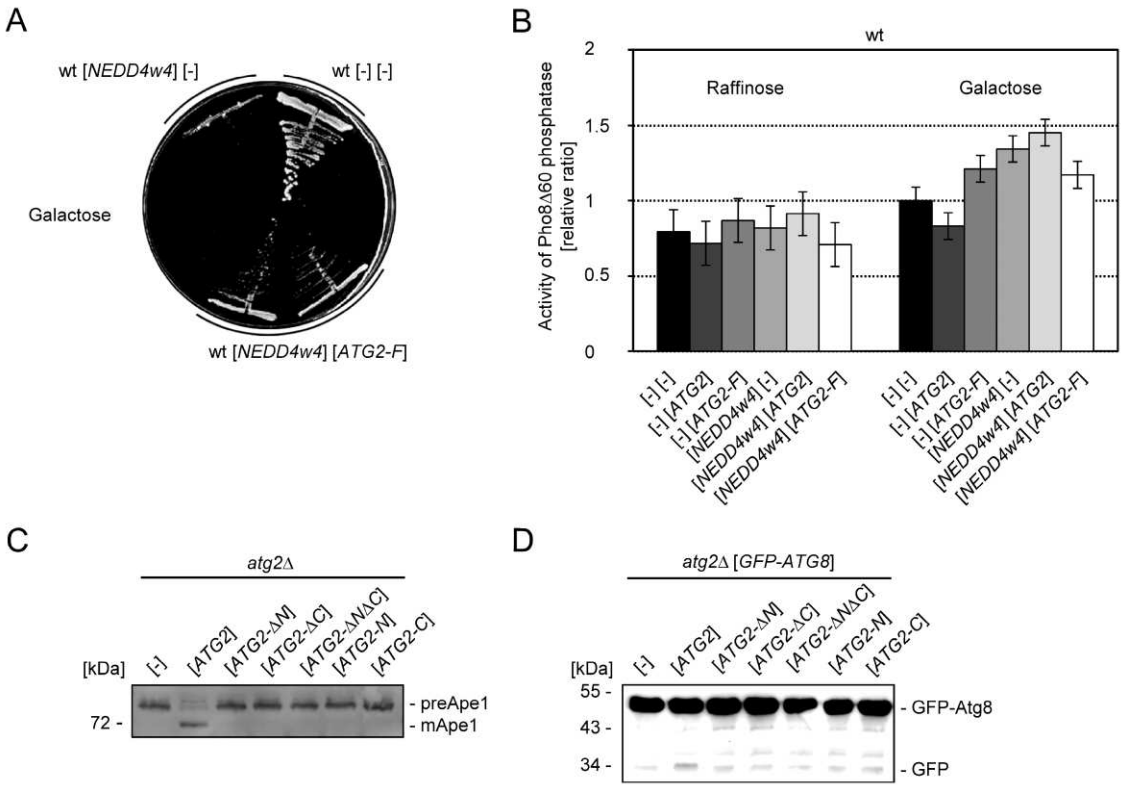

Figure S1. NEDD4w4 and ATG2-F affect cell growth but do not affect nonselective autophagy and fragments of ATG2 do not complement defects of atg2Δ strain in Cvt pathway or nonselective autophagy.

A. Growth of wild type strain (INV) transformed with empty vectors, and wild type strain expressing NEDD4w4 and transformed with empty vector or plasmid bearing fragment of ATG2 (ATG2-F) on SCgal-ura-leu (galactose) plate at 28^{O}C for 5 days.

B. Activity of alkaline phosphatase of pho8Δ60 strain (YPJ2; Romanyuk et al., 2011) transformed with plasmid carrying NEDD4w4 and empty vector or ATG2 or ATG2f fragment. Transformants bearing two empty vectors or expressing ATG2 or ATG2f alone were used as a control. Cells were grown on raffinose-containing medium and shifted to galactose medium for 4 hours. Four independent experiments were performed and means ±SD (standard deviation) are shown.

C. Western blot analysis of preApe1 maturation in atg2Δ strain (BY4741 genetic background) transformed with empty vector or plasmids carrying ATG2, ATG2-ΔN, ATG2-ΔC, ATG2-ΔNΔC, ATG2-N, ATG2-C grown on SC-ura-leu, shifted to nitrogen starvation and analyzed by Western blotting using anti-Ape1 antibody. Wild type strain transformed with empty vector was used as a control.

D. Analysis of GFP-Atg8 degradation. The atg2Δ strain (BY4741) was transformed with plasmid carrying GFP-ATG8 and empty vector or ATG2, ATG2-ΔN, ATG2-ΔC or ATG2-ΔNΔC fragments. Protein extracts were prepared and Western blotting was performed using anti-GFP antibody.

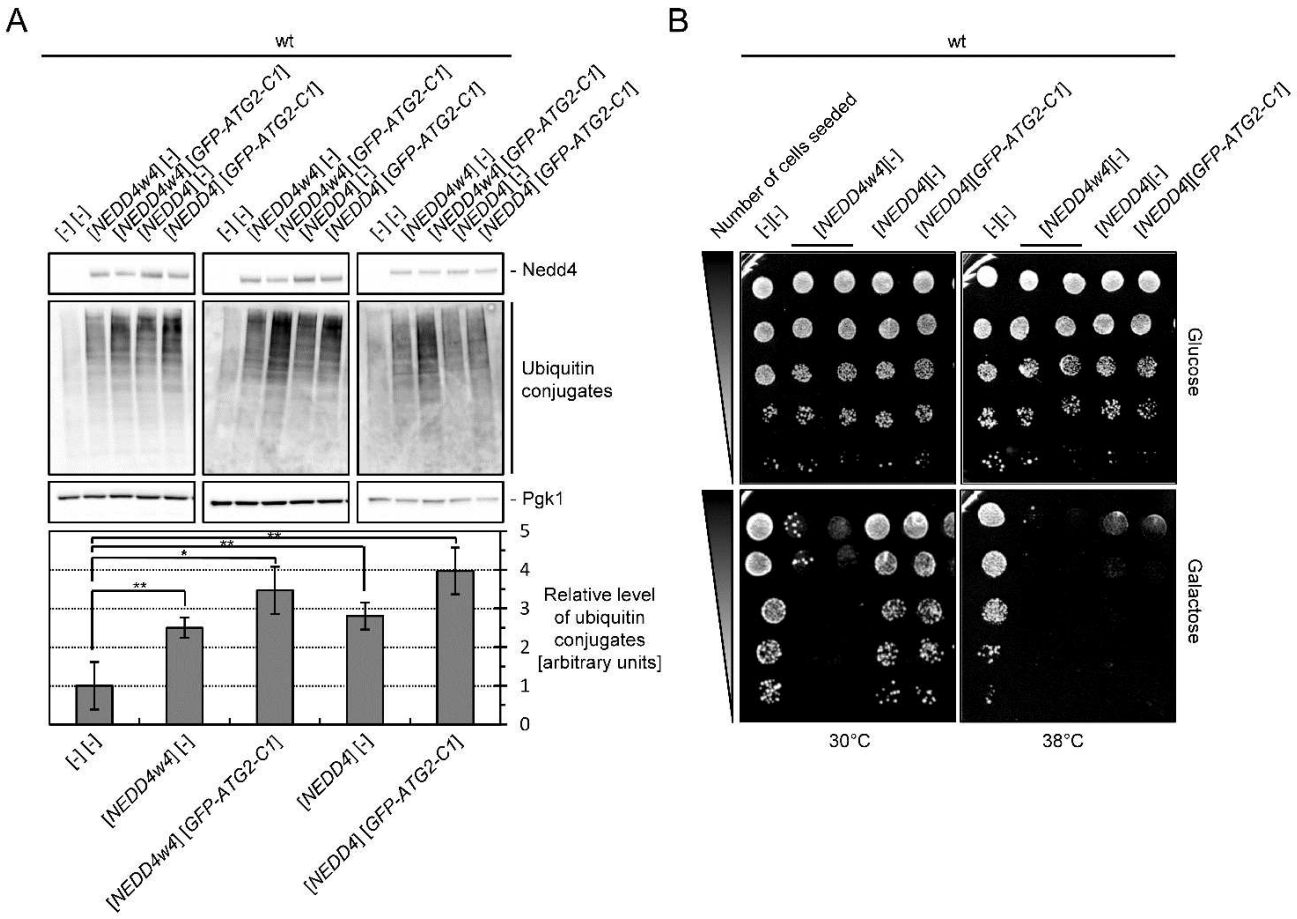

Figure S2. Nedd4 and Nedd4w4 similarly affect the level of ubiquitinated proteins but, in contrast to Nedd4w4, the wild type Nedd4 is not toxic in yeast at 30^{O}C.

A. Wild type **(**BY4741) cells transformed with empty plasmids or plasmids carrying NEDD4, NEDD4w4 or GFP-ATG2-C1 were grown at 30^{O}C in SCraf (raffinose) and transferred to SCgal (galactose) for 3.5 h to induce expression of NEDD4 and NEDD4w4. Protein extracts were prepared by glass beads method. Western blots were developed with anti-ubiquitin, anti-Nedd4 and anti-Pgk1 antibodies. Pgk1 level was used as a loading control. Quantification of results obtained in three independent experiments is shown in the lower panel. The value obtained for wild type strain bearing empty vector was set to 1. Statistical significance level: *, $p<0.02$;
**, $p<0.01$.
B. Growth of transformants as in (**A)** on SC (glucose) and SCgal (galactose) at temperatures indicated. Plates were incubated for 3-5 days.

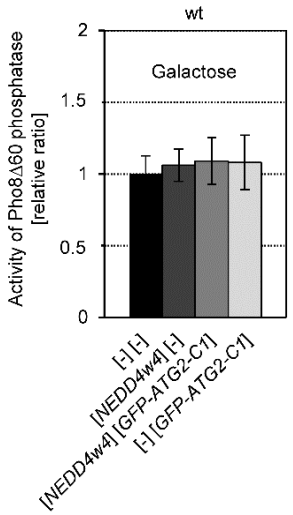

Figure S3. GFP-Atg2-C1 does not induce nonselective autophagy in NEDD4w4-expressing cells.

The pho13Δ pho8Δ60 strain (KJK146, a pho13Δ derivative of TN125; Shintani et al., 2001) was transformed with empty vector or with plasmid bearing NEDD4w4 and with empty vector or GFP-ATG2-C1. Transformants were grown in SCraf-ura-leu at 28^{o}C to OD600 0.4-0.5, then galactose was added to 2% final concentration and cells were grown for additional 4 h. The activity of Pho8Δ60 phosphatase was measured in four independent biological samples of each transformant type and means ±SD (standard deviation) are shown.

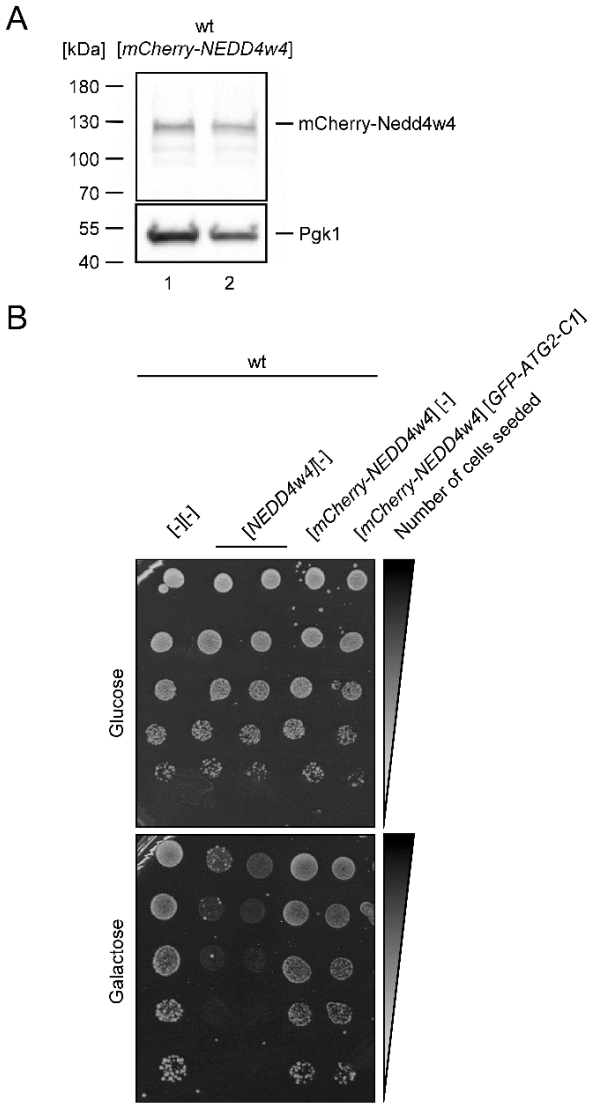

Figure S4. The mCherry-Nedd4w4 is not toxic to yeast.

A. Wild type strain (BY4741) was transformed with plasmid bearing mCherry-NEDD4w4. The level of fusion protein was then analyzed in two independent clones by Western blot using anti-Nedd4 antibody. Pgk1 was used as a loading control.

B. Growth of wild type strain bearing empty vector or vector containing NEDD4w4 or mCherry-NEDD4w4 and the second empty vector or vector containing GFP-ATG2-C1 was checked by drop test on SC (glucose; repression) and SCgal (galactose; induction of NEDD4w4 or mCherry-NEDD4w4 expression) media and the results obtained after incubation at 30^{O}C for 3-7 days are shown.

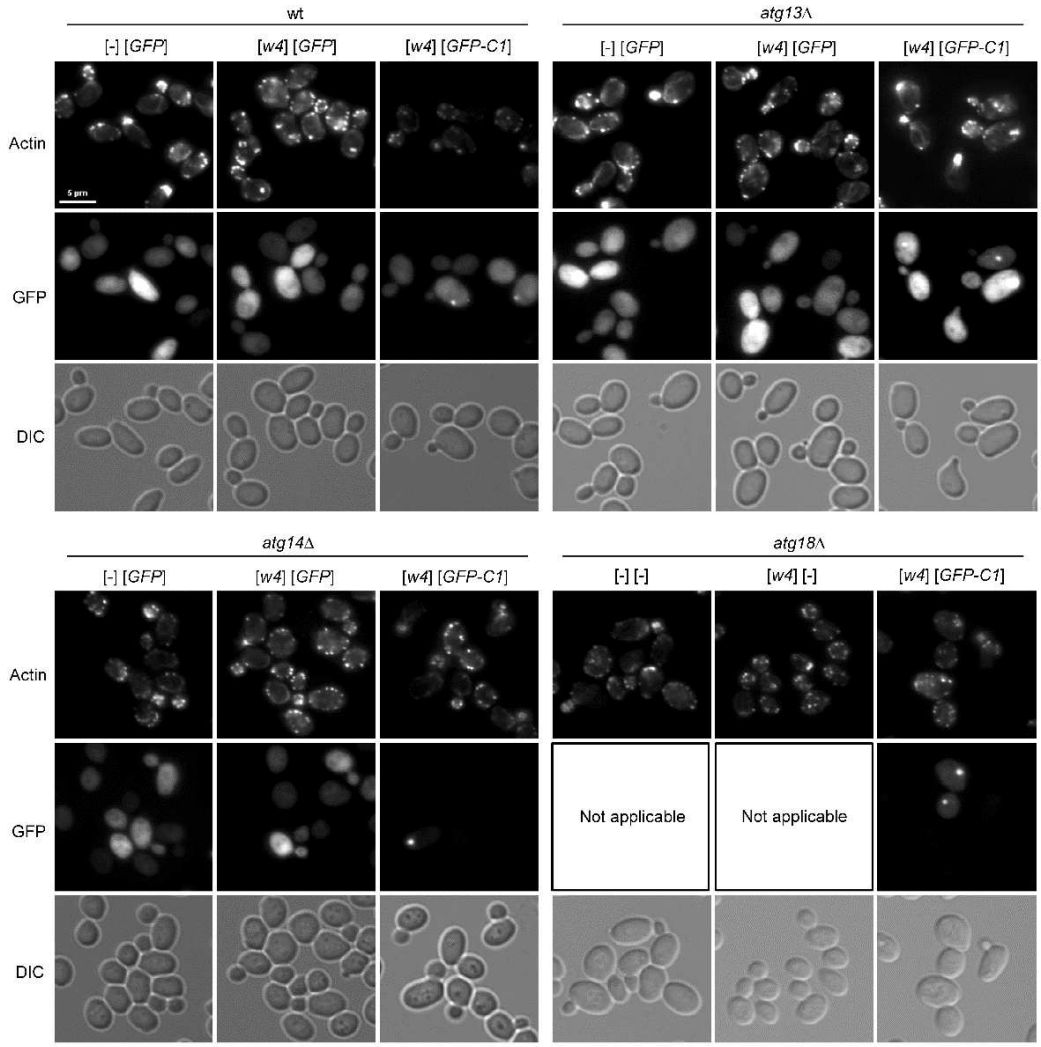

Figure S5. The atg13Δ, atg14Δ and atg18Δ mutations variously affect organization of actin cytoskeleton in cells expressing NEDD4w4 and GFP-ATG2-C1.

Wild type, atg13Δ, atg14Δ and atg18Δ strains (BY4741 genetic background) bearing plasmids carrying NEDD4w4 and GFP-ATG2-C1 were growth to log-phase in SCraf-ura-leu. Expression of NEDD4w4 was induced with galactose for 3.5 h at 28°C. Then cells were fixed using formaldehyde, pelleted, stained for actin filaments using Alexa fluor-conjugated phalloidin and observed using fluorescence microscopy.

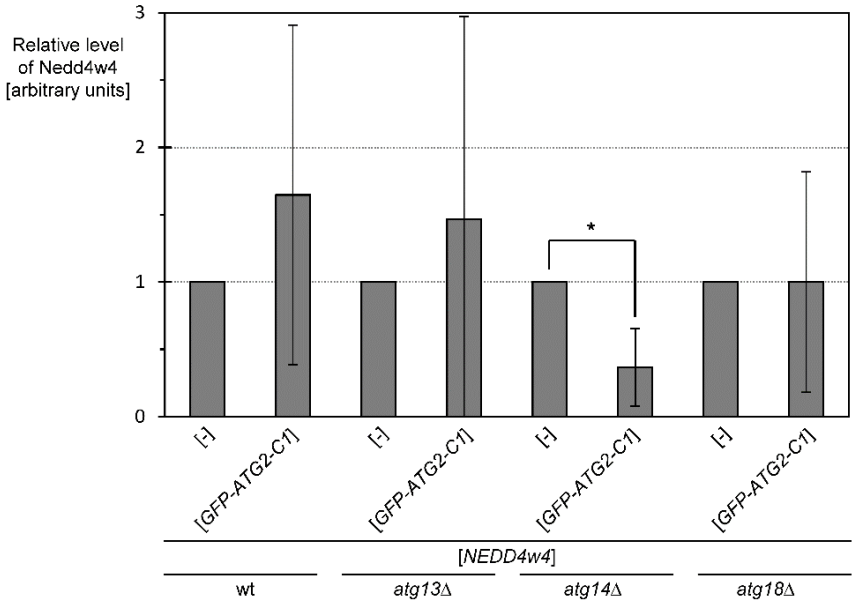

Figure S6. The level of Nedd4 in atg14Δ is affected when GFP-Atg2-C1 is also present.

Wild type, atg13Δ, atg14Δ and atg18Δ strains (in BY4741 background) transformed with empty plasmid or plasmids carrying NEDD4w4 or GFP-ATG2-C1 were grown as in Figure 7. Protein extracts were prepared by glass beads method and analyzed by SDS-PAGE and Western blot. Three independent experiments were performed. Blots were quantified and analyzed statistically, and relative levels of Nedd4w4 normalized to Pgk1 are shown. Statistical significance at $p < 0.02$ level is indicated by an asterisk (*).

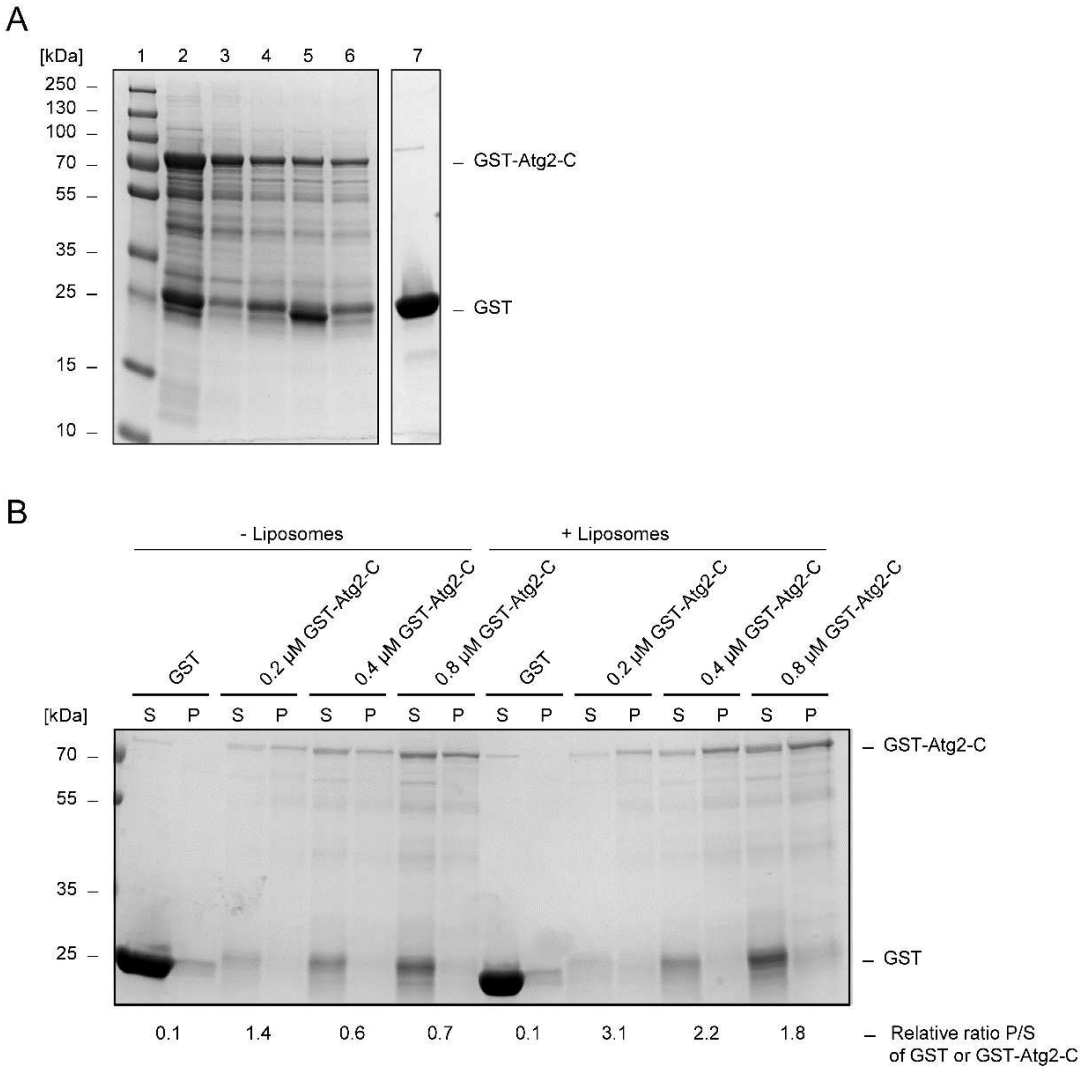

Figure S7. GST-Atg2-C binds to liposomes.

A. E. coli cells bearing pGEX-4T-GST-ATG2-C plasmid were grown at 37°C and induced with IPTG at 30°C for 7 h. GST-Atg2-C was purified using glutathione-sepharose beads and eluted with reduced glutathione. Buffer was exchanged using PD Minitrap G-25 columns. Known amounts of actin were used as a marker to estimate the amount of purified protein. 1. Molecular weight marker; 2. Beads after binding of Atg2-C; 3. Beads after elution of GST-Atg2-C; 4. Elution; 5, 6. Elution after buffer exchange; 7. GST purified in the same way.
B. GST-Atg2-C protein at concentration indicated or GST were incubated with liposomes or with lipid buffer alone and sedimented at 250 000 × g for 15 min. Pellets (P) and supernatants (S) were analyzed by SDS-PAGE and stained with Coomassie Brilliant Blue. Intensity of GST-Atg2-C bands in each fraction was measured densitometrically using Image Lab software and P/S ratio is shown.

SUPPLEMENTARY REFERENCES

Chacinska, A., Szczesniak, B., Kochneva-Pervukhova, N. V., Kushnirov, V. V., Ter-Avanesyan, M. D., Boguta, M. (2001) Ssb1 chaperone is a [PSI+] prion- curing factor. Curr Genet. 39, 62-7.

Gajewska, B., Shcherbik, N., Oficjalska, D., Haines, D. S., Zoladek, T. (2003) Functional analysis of the human orthologue of the RSP5-encoded ubiquitin protein ligase, hNedd4, in yeast. Curr Genet. 43, 1-10.

Gietz, R. D., Sugino, A. (1988) New yeast-Escherichia coli shuttle vectors constructed with in vitro mutagenized yeast genes lacking six-base pair restriction sites. Gene. 74, 527-34.

Hill, J. E., Myers, A. M., Koerner, T. J., Tzagoloff, A. (1986) Yeast/E. coli shuttle vectors with multiple unique restriction sites. Yeast. 2, 163-7.

Noda T, Matsuura A, Wada Y, Ohsumi Y (1995) Novel system for monitoring autophagy in the yeast Saccharomyces cerevisiae. Biochem Biophys Res Commun 210, 126-132.

Romanyuk, D., Polak, A., Maleszewska, A., Sienko, M., Grynberg, M., Zoladek, T. (2011) Human hAtg2A protein expressed in yeast is recruited to preautophagosomal structure but does not complement autophagy defects of atg2Δ strain. Acta Biochim Pol. 58, 365-74.

Shintani, T., Suzuki, K., Kamada, Y., Noda, T., Ohsumi, Y. (2001) Apg2p functions in autophagosome formation on the perivacuolar structure. J Biol Chem. 276, 30452-60.

Suzuki, K., Kirisako, T., Kamada, Y., Mizushima, N., Noda, T., Ohsumi, Y. (2001) The pre-autophagosomal structure organized by concerted functions of APG genes is essential for autophagosome formation. EMBO J 20,